Received: 3 March 2021 | Revised: 4 August 2021 | Accepted: 9 August 2021

DOI: 10.1002/cne.25232

RESEARCH ARTICLE

JCN RESEARCH IN SYSTEMS NEUROSCIENCE THE JOURNAL OF COMPARATIVE NEUROLOGY WILEY

Morphological and neurochemical characterization of glycinergic neurons in laminae I–IV of the mouse spinal dorsal horn

Camila Oliveira Miranda[1] | Krisztina Hegedüs[1] | Hendrik Wildner[2] | Hanns Ulrich Zeilhofer[2,3] | Miklós Antal[1]

[1]Department of Anatomy, Histology and Embryology, Faculty of Medicine, University of Debrecen, Debrecen, Hungary

[2]Institute of Pharmacology and Toxicology, University of Zurich, Zurich, Switzerland

[3]Institute of Pharmaceutical Sciences, Swiss Federal Institute of Technology, Zurich, Switzerland

Correspondence
Miklós Antal, Department of Anatomy, Histology and Embryology, Faculty of Medicine, University of Debrecen, Nagyerdei krt 98., 4032 Debrecen, Hungary.
Email: antal@anat.med.unideb.hu

Funding information
Hungarian Academy of Sciences, Grant/Award Number: MTA-TKI 242; Hungarian National Brain Research Program, Grant/Award Number: KTIA_NAP_13-1-2013-0001; Swiss National Science Foundation, Grant/Award Number: 310030197888

Abstract

A growing body of experimental evidence shows that glycinergic inhibition plays vital roles in spinal pain processing. In spite of this, however, our knowledge about the morphology, neurochemical characteristics, and synaptic relations of glycinergic neurons in the spinal dorsal horn is very limited. The lack of this knowledge makes our understanding about the specific contribution of glycinergic neurons to spinal pain processing quite vague. Here we investigated the morphology and neurochemical characteristics of glycinergic neurons in laminae I–IV of the spinal dorsal horn using a GlyT2::CreERT2-tdTomato transgenic mouse line. Confirming previous reports, we show that glycinergic neurons are sparsely distributed in laminae I–II, but their densities are much higher in lamina III and especially in lamina IV. First in the literature, we provide experimental evidence indicating that in addition to neurons in which glycine colocalizes with GABA, there are glycinergic neurons in laminae I–II that do not express GABA and can thus be referred to as glycine-only neurons. According to the shape and size of cell bodies and dendritic morphology, we divided the tdTomato-labeled glycinergic neurons into three and six morphological groups in laminae I–II and laminae III–IV, respectively. We also demonstrate that most of the glycinergic neurons co-express neuronal nitric oxide synthase, parvalbumin, the receptor tyrosine kinase RET, and the retinoic acid-related orphan nuclear receptor β (RORβ), but there might be others that need further neurochemical characterization. The present findings may foster our understanding about the contribution of glycinergic inhibition to spinal pain processing.

KEYWORDS
cell morphology, glycine transporter 2, glycinergic neurons, immunohistochemistry, mouse, spinal dorsal horn

1 | INTRODUCTION

Neural circuits in the spinal dorsal horn play a fundamental role in the processing of neural activities evoked by peripheral noxious stimuli. In case of peripheral inflammation and neuropathy, becomes perturbed and shifted toward stronger excitation, thereby contributing to central sensitization and chronic pain (for review, see Peirs & Seal, 2016; Koch et al., 2018; Zeilhofer et al., 2021). Furthermore, a loss of inhibition at the border between the superficial and the deep dorsal horn activates normally silent polysynaptic projections from non-nociceptive touch sensitive Aβ fibers to nociceptive projections neurons of lamina I, thereby giving rise to allodynia (touch-evoked pain), which is a hallmark of many chronic pain syndromes. Thus, elucidating the nature of inhibitory control over the incoming nociceptive signals is crucial for the understanding of spinal pain processing, the consecutive development of chronic pain, and revealing possibilities for pain attenuation strategies, which may take effect at the level of the spinal dorsal horn.

Fast inhibitory neurotransmission is mediated by both GABA and glycine in the spinal cord. Early immunocytochemical studies showed that in the superficial spinal dorsal horn, glycine is present exclusively in cells and axon terminals, which contain GABA (Todd, 1996; Todd et al., 1995, 1996; Todd & Sullivan, 1990), but only half of the GABAergic cells have been found to be immunoreactive also for glycine (Mitchell et al., 1993; Todd & Sullivan, 1990). Thus, while recording miniature inhibitory postsynaptic currents (mIPSCs) from neurons within the superficial spinal dorsal horn, one would expect that cells displaying glycine receptor-mediated mIPSCs would also show $GABA_A$ receptor-mediated mIPSCs. On the contrary, however, glycine-only mIPSCs were detected in many cases from superficial dorsal horn neurons (Chery & de Koninck, 1999; Keller et al., 2001). Following these early observations, the importance of glycine-only synaptic inhibition in spinal pain control has been substantiated by many other reports (Aubrey & Supplisson, 2018; Lu et al., 2015). It seems that a substantial proportion of the inhibitory input onto neurons in the superficial spinal dorsal horn, especially in laminae IIi and III, is glycinergic (Foster et al., 2015; Lu et al., 2015; Punnakkal et al., 2014; Takazawa et al., 2017; Takazawa & McDermott, 2010), and the ablation or silencing of glycinergic synaptic transmission induces thermal and mechanical sensitization and spontaneous pain (Foster et al., 2015; Lu et al., 2015).

Although it is now widely accepted that glycinergic neurons play an important role in spinal pain processing, the axonal and dendritic morphology of dorsal horn glycinergic neurons as well as the definition of their presynaptic input neurons and postsynaptic targets are still ill-defined. With the exception of some early studies in which glycine immunoreactivity was identified in some Golgi impregnated neurons (Powell & Todd, 1992; Todd & Sullivan, 1990), there is no report about the morphology and neurochemical characterization of glycinergic neurons in the spinal dorsal horn. Without this fundamental knowledge, however, the contribution of glycinergic inhibition to spinal pain processing cannot be accurately described. Thus, in a series of experiments we intend to explore the distribution and morphological properties as well as the synaptic relations of glycinergic neurons in the superficial spinal dorsal horn. As the first piece of these studies, we present an account about the distribution, dendritic morphology, and neurochemical characterization of glycinergic neurons in laminae I–IV of the spinal dorsal horn in a transgenic mouse line, in which glycinergic neurons were labeled with tdTomato under the control of the glycine transporter 2 (GlyT2) gene, encoding a highly specific axonal membrane transporter of glycinergic neurons (Poyatos et al., 1997).

2 | MATERIALS AND METHODS

2.1 | Animals

A bacterial artificial chromosome (BAC) transgenic mouse expressing an estrogen receptor-dependent CreERT2 recombinase under the transcriptional control of the GlyT2 gene (GlyT2::CreERT2) was generated using the same strategy previously used to generate GlyT2::Cre (Foster et al., 2015) and GlyT2::eGFP (Zeilhofer et al., 2005) mice. The GlyT2::CreERT2 mice were crossed with a tdTomato reporter mice (007914—B6.Cg-*Gt(ROSA)26Sor*$^{tm14(CAG-tdTomato)Hze}$/J, The Jackson Laboratories, Bar Harbor, ME, USA). Double transgenic off-springs of these mouse lines received an intraperitoneal tamoxifen injection (2 mg/pup, Sigma, Cat# T5648) at the 8th–10th postnatal days. The tamoxifen solution was prepared according to Zheng et al. (2019). At the 18th–20th postnatal days, the animals were genotyped for both the GlyT2ERT2 and the tdTomato transgene, and only those male animals were kept for the experiments that expressed both genes. These animals grew up and nine of them were used for the experiments at the age of 3–5 months. All animal study protocols were approved by the Animal Care and Protection Committee at the University of Debrecen and were in accordance with the European Community Council Directives.

2.2 | Preparation of tissue sections

2.2.1 | For immunohistochemistry

Animals were deeply anesthetized with sodium pentobarbital (50 mg/kg, i.p.) and transcardially perfused with Tyrode's solution (oxygenated with a mixture of 95% O_2, 5% CO_2), followed by a fixative containing 4% paraformaldehyde dissolved in .1 M phosphate buffer (PB, pH 7.4). After the transcardial fixation, the lumbar segments of the spinal cord were removed, post-fixed in the original fixative for 3–4 hours, and immersed into 10 and 20% sucrose dissolved in .1 M PB until they sank. In order to enhance reagent penetration, the removed spinal cord was freeze-thawed in liquid nitrogen, sectioned at 50 or 100 μm on a vibratome, and extensively washed in .1 M PB. While the 50-μm thick sections were obtained in transverse, horizontal, and sagittal directions, the 100 μm thick sections were always cut in sagittal orientation. The 100 μm thick sections were mounted on glass slides without any further treatment, dehydrated, and covered with Permount neutral medium; whereas the 50-μm thick sections were further processed for immunohistochemistry.

2.2.2 | For in situ hybridization

Animals were deeply anesthetized with sodium pentobarbital (50 mg/kg, i.p.). The lumbar segments of the spinal cord were removed and frozen on dry ice. The frozen spinal cord was cut into 16-μm thick sections in a cryostat and mounted onto Superfrost Plus glass sides (Thermo Fischer Scientific, Cat# J1800AMNZ). The sections were stored on −20°C until further treatments.

2.3 | Immunohistochemistry

2.3.1 | Single immunostaining

A single immunostaining protocol was performed to study the expression of markers specific for inhibitory neurons (Boyle et al., 2017; Smith et al., 2015) in GlyT2::CreERT2-tdTomato-labeled neurons. Free-floating sections were incubated with one of the following antibodies: (1) rabbit anti-paired box gene 2 transcription factor (PAX2) (diluted 1:1000, Thermo Fisher Scientific Cat# 71-6000, RRID:AB_2533990), (2) goat anti-neuronal nitric oxide synthase (nNOS) (diluted 1:8000, Abcam Cat# ab1376, RRID:AB_1566510), (3) rabbit anti-neuropeptide Y (NPY) (1:400, ABCAM Cat# AB30914, RRID:AB_2807030), (4) rabbit anti-parvalbumin (PV) (diluted 1:60,000, Swant Cat# PV27, RRID: AB_2631173) or mouse anti-PV (diluted 1:20,000, Swant Cat# PV235, RRID:AB_10000393), (5) rabbit anti-galanin (diluted 1:12000, Peninsula Laboratories Cat# T-4334.0050, RRID:AB_518348), and (6) goat anti-calretinin (diluted 1:30,000, Swant Cat# CG1, RRID:AB_10000342). The sections were incubated in the primary antibody solutions for 2 days at 4°C and were transferred for an overnight treatment into goat anti-rabbit IgG, goat anti-mouse IgG, or rabbit anti-goat IgG secondary antibodies conjugated with Alexa Fluor 488 (diluted 1:1000, Thermo Fisher Scientific Cat# A-11008, RRID:AB_143165;;Cat # A-11001, AB_2534069; Cat# A-11078, RRID: AB_2534122). Before the antibody treatments, the sections were kept in 20% normal goat or normal rabbit serum (Vector Laboratories, Burlingame, CA, USA) for 50 min. Antibodies were diluted in 10 mM TPBS (pH 7.4) to which 1% normal goat or rabbit serum (Vector Laboratories., Burlingame, CA, USA) was added. Sections were mounted on glass slides and covered with Vectashield mounting medium (Vector Laboratories., Burlingame, CA, USA).

2.3.2 | Double immunostaining

Double-immunostaining protocols were performed to study the colocalization of glycinergic and GABAergic markers, GlyT2, and glutamic acid decarboxylase (GAD), respectively, in axon terminals of GlyT2:: CreERT2-tdTomato-labeled neurons in laminae I–II. Free-floating sections were incubated with a mixture of guinea pig anti-GlyT2 (1:1000, Synaptic Systems Cat# 272004, RRID:AB_2619998) and rabbit anti-GAD recognizing both 65kD and 67 kD isoforms of the enzyme (GAD65/67) (diluted 1:2000, Abcam, Cat# AB183999, EPR19366). The sections were incubated in the primary antibody solutions for 2 days at 4°C and were transferred for an overnight treatment into a mixture of goat anti-guinea pig IgG conjugated with Alexa Fluor 488 (diluted 1:1000, Thermo Fisher Scientific Cat# A-11073, RRID:AB_2534117) and goat anti-rabbit IgG conjugated with Alexa Fluor 647 (diluted 1:1000, Thermo Fisher Scientific Cat# A-21244, RRID:AB_2535812). Before the antibody treatments, the sections were kept in 20% normal goat serum (Vector Laboratories., Burlingame, CA, USA) for 50 min. Antibodies were diluted in 10 mM TPBS (pH 7.4) to which 1% normal goat serum (Vector Laboratories., Burlingame, CA, USA) was added. Sections were mounted on glass slides and covered with Vectashield mounting medium (Vector Laboratories., Burlingame, CA, USA).

2.4 | Characterization of antibodies

Primary antibodies used in this study are listed in Table 1.

2.4.1 | Anti-calretinin

The calretinin (CR) antibody was produced against recombinant human CR and showed no staining in the brains of CR-knockout mice (manufacturer's specification).

2.4.2 | Anti-GAD65/67

This is a recombinant monoclonal antibody raised against the aa 450 to the C-terminus fragment of mouse GAD65+GAD67. The

TABLE 1 List of primary antibodies used

Target	Host species	Dilution	Catalog #	Company	RRID
Calretinin	Goat	1:30000	CG1	SWANT	AB_10000342
GAD65/67	Rabbit	1:2000	AB183999	ABCAM	EPR19366
Galanin	Rabbit	1:12000	T4334	Peninsula	AB_518348
GlyT2	Guinea pig	1:1000	272-004	Synaptic System	AB_2619998
nNOS	Goat	1:8000	AB1376	ABCAM	AB_300614
Neuropeptide Y	Rabbit	1:400	AB30914	ABCAM	AB_1566510
Parvalbumin	Rabbit	1:60000	PV27	SWANT	AB_2631173
Parvalbumin	Mouse	1:20000	PV235	SWANT	AB_10000393
PAX2	Rabbit	1:1000	71–6000	ThermoFisher Sci.	AB_2533990

antibody was extensively tested with Western blots and various immunostaining protocols, and it was shown that it specifically recognizes both the 65 and 67 kDa isoforms of GAD (Augustine et al., 2018; Ikegami et al., 2018).

2.4.3 | Anti-galanin

The antibody was raised against a synthetic peptide (GWTLNSAGYLLGPHAIDNHRSFSDKHGLT; sequence from rat galanin (GAL)). It has been shown that preincubation of the antibody with the immunizing peptide blocks all immunolabeling (Landry et al., 2006; Simmons et al., 1995).

2.4.4 | Anti-GlyT2

The anti-GlyT2 antibody was raised against a rat N-terminus 229-aa peptide and validated by Western blot, reflecting a pattern and distribution consistent with previous spinal cord staining (Corleto et al., 2015; Tulloch et al., 2019).

2.4.5 | Anti-nNOS

The antibody was raised against a synthetic peptide corresponding to amino acids 1423–1434 of human nNOS. The specificity of the antibody was tested by Western blot and immunohistochemical staining carried out on human brain tissue lysates and mouse dorsal root ganglion following spinal nerve ligation, respectively (manufacturer's specification).

2.4.6 | Anti-NPY

It has been shown that immunostaining with the NPY antibody is abolished by preincubation with NPY (Rowan et al., 1993). It has been reported also that immunostaining with an antibody raised in sheep is absent in the brains of NPY knockout mice (Glavas et al., 2008). In addition, it was found that dual immunofluorescence staining with the rabbit and sheep NPY antibodies revealed identical structures within the dorsal horn (Polgar et al., 2011).

2.4.7 | Anti-parvalbumin

The polyclonal rabbit PV antiserum was raised against recombinant rat PV. In Western blot, a single band at the molecular weight level of PV (~12 kDa) was detected by the antibody in brain extracts form wild-type (WT) animals while no signal was detected in extracts from PV-KO mice (Filice et al., 2017). In immunofluorescent studies, the antibody labels subpopulations of neurons with high efficacy in WT animals, but does not stain any neurons in the brain of knockout mice.

The mouse monoclonal PV antibody is one of the most widely used PV antisera in studies of the central nervous system. The immunogen used to generate the antibody was carp-II PV. The specificity of this antibody has been well documented (Celio et al., 1988).

2.4.8 | Anti-PAX2

The antibody was raised from a GST-Pax2 fusion protein derived from the C-terminal domain (aa 188–385) of the murine Pax2 protein (Dressler & Doughlass, 1992). Western blot with mouse embryonic kidney lysates revealed two bands: a major band at 46 kDa (Pax2b) and a minor band at 48 kDa (Pax2a), representing two isoforms of Pax2 from alternative splicing (Dressler & Doughlass, 1992). The specificity of the antibody has also been confirmed in immunohistochemical protocols (Ikenaga et al., 2011; Kim et al., 2011).

2.5 | Confocal microscopy

Single and long series of 1 μm thick optical sections were scanned with an Olympus FV3000 confocal microscope from the immunostained sections. Scanning was carried out using a 40x oil-immersion lens (NA: 1.3). The confocal settings (laser power, confocal aperture, and gain) were identical for all sections, and care was taken to ensure that no pixels corresponding to puncta immunostained for the markers were saturated. The scanned images were processed by Adobe Photoshop CS5 software.

2.6 | Neurolucida reconstruction

The long series of scanned images were transferred to a Neurolucida system (Neurolucida v.11.07, MicroBrightfied Bioscience, Williston, VT, USA) with the aid of which the cell bodies and the dendritic trees of tdTomato-labeled neurons were reconstructed from the image stacks in three dimensions. For making illustrations from the reconstructions, we rotated the neurons into a rostro/caudal-dorso/ventral orientation and made a two-dimensional compressed image from the three-dimensional dendritic tree.

2.7 | Multiplex in situ hybridization

For multiplex fluorescent in situ hybridization (FISH), the manual RNAScope® Multiplex Fluorescent Assay (ACD, Biotechne, catalog # 320850) was used. The manufacturer's pretreatment protocol for fresh frozen tissue (document no. 320513, rev. date: November 5, 2015) and detection protocol (document no. 320293-UM, rev. date: March 14, 2017) were followed. The following probes were used: Slc6a5 (GlyT2) (ACD, Biotechne, Cat# 409741-C3), tdTomato (ACD, Biotechne, Cat# 317041 and 317041-C2), the retinoic acid-related

orphan nuclear receptor β (RORβ) (ACD, Biotechne, Cat# 444271-C3), and the receptor tyrosine kinase RET (ACD, Biotechne, Cat# 431791). The reaction end-product of the tdTomato probes appeared in red, whereas all others appeared in green. Sections were covered with Vectashield mounting medium containing DAPI (Vector Laboratories., Burlingame, CA, USA). Sections were investigated with an LSM 800 confocal microscope and short series of 1.5-μm thick confocal sections with 50% overlap were photographed using a 25x lens (NA: .8).

2.8 | Statistical analysis

The colocalization of GlyT2::CreERT2-tdTomato labeling with the expression of markers specific for cell bodies and/or axon terminals of inhibitory neurons was quantitatively analyzed in the immunostained sections.

2.8.1 | Expression of markers within the cell bodies of GlyT2::CreERT2-tdTomato-labeled neurons

The colocalization of GlyT2::CreERT2-tdTomato labeling with the expression of PAX2, nNOS, NPY, GAL, PV, caltretinin, GlyT2, RORβ, and RET was investigated this way. Cell bodies labeled with tdTomato and/or immunostained for PAX2, nNOS, NPY, GAL, PV, CR, and/or giving positive hybridization signal for GlyT2, RORβ, and RET were identified and counted in laminae of the dorsal horn where the immunostaining for the marker was observed. Percentage of tdTomato-labeled neurons, which was also labeled for the marker, was calculated.

The colocalization for all investigated markers was analyzed in three animals. Five sections from each animals were randomly selected and the quantitative measurement was carried out within the whole area which was immunostained for the marker. Thus, the calculation of quantitative figures in each case was based on the investigation of 15 independent sections.

2.8.2 | Expression of markers within the axon terminals of GlyT2::CreERT2-tdTomato-labeled neurons

The colocalization of the GlyT2::CreERT2-tdTomato labeling with immunostaining for GlyT2 and GAD as well as the colocalization between GlyT2 and GAD immunostaining were investigated. Because of the limited penetration of the anti-GlyT2 and anti GAD65/67 antibodies into the sections, first we found a confocal layer within which the staining for both GlyT2 and GAD65/67 was strong. For this reason, we obtained the confocal images in the very superficial layer of the sections, not deeper than 2–3 μm from the surface. The immunostained profiles were counted manually, according to the following way: A 10 × 10 standard square grid in which the edge-length of the unit square was 5 μm was placed onto the regions of confocal images corresponding to laminae I–II of the superficial spinal dorsal horn. The proper placement of the grid was based on the following criteria: (1) The border between the dorsal column and the dorsal horn was easily identified on the basis of the intensity of immunostaining and (2) The border between laminae II and III was approximated on the basis of previous observations (McClung & Castro, 1978; McNeil et al., 1988; Molander et al., 1984). It has been repeatedly demonstrated in ultrastructural studies that there are almost no myelinated axons in lamina II, while they are abundant in lamina III. Thus, the border between laminae II and III can be defined quite precisely in ultrastructural studies, and the thickness of laminae I–II can be measured. For this reason, tdTomato labeling and immunoreactivities as well as colocalizations were investigated in the most superficial 60-μm thick zone of the dorsal horn that had earlier been identified as layers corresponding to laminae I–II in the L4–L5 segments of the mouse spinal dorsal horn (Sengul et al., 2013).

Profiles that showed tdTomato labeling or immunoreactivity for GlyT2 or GAD65/67 over the edges of all 5 μm unit squares were counted. The selected profiles were then examined in two different ways. (1) We determined whether (a) the tdTomato-labeled profiles were also immunoreactive for GlyT2 and (b) the profiles double labeled for tdTomato and GlyT2 were also immunoreactive for GAD. (2) We examined the GAD65/67 immunostaining in GlyT2-positive axon terminals, regardless whether they were labeled with tdTomato or not. Because the GlyT2 antibody utilized in the present study was raised against the intracellular domain of the transporter, in case of colocalization, the GlyT2 immunolabeled puncta were expected to be located within the confines of the area labeled with tdTomato. The colocalizations were analyzed in three animals. Three sections from each animals were randomly selected and the quantitative measurement was carried out in a regions of interest (ROI) that was randomly selected from each section. Thus, the calculation of quantitative figures in each case was based on the investigation of nine ROIs. Mean values and standard error of means (*SEM*) were calculated.

3 | RESULTS

3.1 | Distribution of GlyT2:CreERT2-tdTomato labeling in laminae I–IV of the spinal dorsal horn

Investigating the dorsal horn at the level of the lumbar spinal segments of GlyT2:CreERT2-tdTomato mice, we found a robust labeling in laminae I–IV. tdTomato labeling was observed in cell bodies and also in processes arising from the cell bodies (Figure 1a). Elongated labeled profiles resembling dendrites and/or interbouton segments of axons were also frequently seen (Figure 1a). The image, however, was dominated by a diffuse punctate labeling, which appeared throughout laminae I–IV (Figure 1a) with a more or less homogeneous density. Although labeled cell bodies were seen only occasionally in lamina II, and their numbers were only slightly higher in lamina I (Figure 1b,c), the punctate labeling was very strong even in these two superficial laminae of the dorsal horn (Figure 1a) suggesting that glycinergic neurons of the deep dorsal horn had dendrites and/or axons extending to

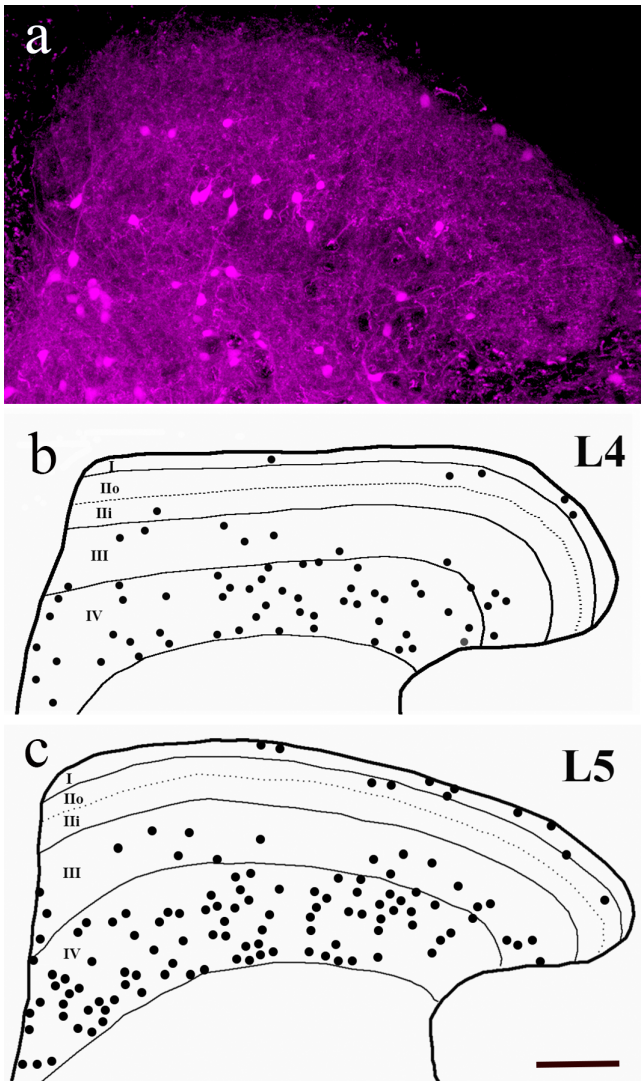

FIGURE 1 Distribution of GlyT2::CreERT2-tdTomato labeling in the spinal dorsal horn. (a) Micrograph of a single confocal section showing an abundant tdTomato labeling of cell bodies, dendrites, and axonal profiles in the dorsal horn of L6 lumbar segment. (b, c) Schematic representation of the distribution of labeled cell bodies at the level of L4 and L5 segments in laminae I–IV of the spinal gray matter. Labeled cells were collected from an approximately 500-μm long pieces of the L4 and L5 spinal segments. The contour of the spinal gray matter and the borders among the adjacent laminae are illustrated according to Sengul et al. (2013). Bar: 100 μm [Color figure can be viewed at wileyonlinelibrary.com]

the superficial dorsal horn. Labeled neurons were found in much higher numbers in lamina III, whereas they showed a remarkably high density in lamina IV (Figure 1b,c).

3.2 | Pax2, GlyT2, and GAD expression in GlyT2::CreERT2-tdTomato-labeled neuronal profiles

Although GlyT2:CreERT2 genetic construct was generated using the same strategy previously used to generate GlyT2::Cre (Foster et al., 2015) and GlyT2::eGFP (Zeilhofer et al., 2005), and the specificity of GlyT2::Cre and GlyT2::eGFP constructs was very carefully tested (Foster et al., 2015; Zeilhofer et al., 2005), before any further evaluation of the tdTomato labeling, we verified that tdTomato expression in GlyT2::CreERT2;tdTomato double transgenic mice was specific for glycinergic neurons. Thus first, we investigated the expression of Pax2, a transcription factor frequently used as a reliable marker of inhibitory interneurons in the spinal cord (Alaynick et al., 2011; Balázs et al., 2017), in perikarya of tdTomato-labeled neurons (Figure 2a–c). In the nine investigated sections, 183 tdTomato-labeled cell bodies were found in laminae I–IV of which 97.35 ± 2.38% were stained also for Pax2. Thus, tdTomato-labeled cells in the spinal dorsal horn can be regarded as inhibitory neurons. Second, to define whether these inhibitory neurons were indeed glycinergic, we performed multiplex FISH to detect mRNAs coding tdTomato and GlyT2 (Figure 2d–e). All of the 152 tdTomato mRNA-positive cells, which we found in laminae I–IV, showed also positive hybridization signal for GlyT2 mRNA. This finding clearly indicates that crossing the GlyT2::CreERT2 animals with the tdTomato reporter mice resulted in tdTomato labeling that was highly specific for glycinergic neurons.

Next, we investigated whether these inhibitory cells belong to the group of glycinergic neurons that are also GABAergic (Mitchell et al., 1993; Todd & Sullivan, 1990) or represent a glycine-only subpopulation of inhibitory neurons (Aubrey & Supplisson, 2018; Foster et al., 2015; Lu et al., 2015; Takazawa et al., 2017). For this reason, we double immunostained sections obtained from the GlyT2::Cre-tdTomato animals with anti-GlyT2 and anti-GAD65/67 antibodies and investigated the colocalization between tdTomato labeling and GlyT2 as well as GAD65/67 immunostaining in 1-μm thick single confocal optical sections (Figure 3). Because of the high densities of tdTomato-labeled cell bodies and dendrites in laminae III–IV, we carried out this study only in laminae I–II where the relative proportion of tdTomato-labeled axon terminals was much higher than that of dendrites. In the nine ROIs, we counted 105 tdTomato-labeled puncta, 62.12 ± 3.94% of which were immunostained for GlyT2 (Table 2). Investigating the GAD65/67 expression in those tdTomato-labeled profiles that were immunostained for GlyT2, we found that 45.49 ± 3.84% of GlyT2-positive puncta were also immunostained for GAD65/67 (Table 2). However, GAD65/67 was virtually absent in the GlyT2-negative tdTomato-labeled profiles. Only four (3.80%) of them were immunostained for GAD. Thus, tdTomato-positive but GlyT2- and GAD-negative profiles may represent dendrites and/or inter-bouton segments of axons.

To validate the existence of glycine-only axon terminals in laminae I–II, we examined the GAD65/67 immunostaining in GlyT2-positive axon terminals regardless whether they were labeled with tdTomato or not. This way, we counted 123 axon terminals immunostained for GlyT2 and found that only 46.02 ± 4.22% of them was stained also for GAD65/67 (Table 2).

The findings indicate that the tdTomato-labeled neurons in the superficial spinal dorsal horn of the GlyT2::CreERT2-tdTomato animals are glycinergic inhibitory neurons. Many of their axon terminals

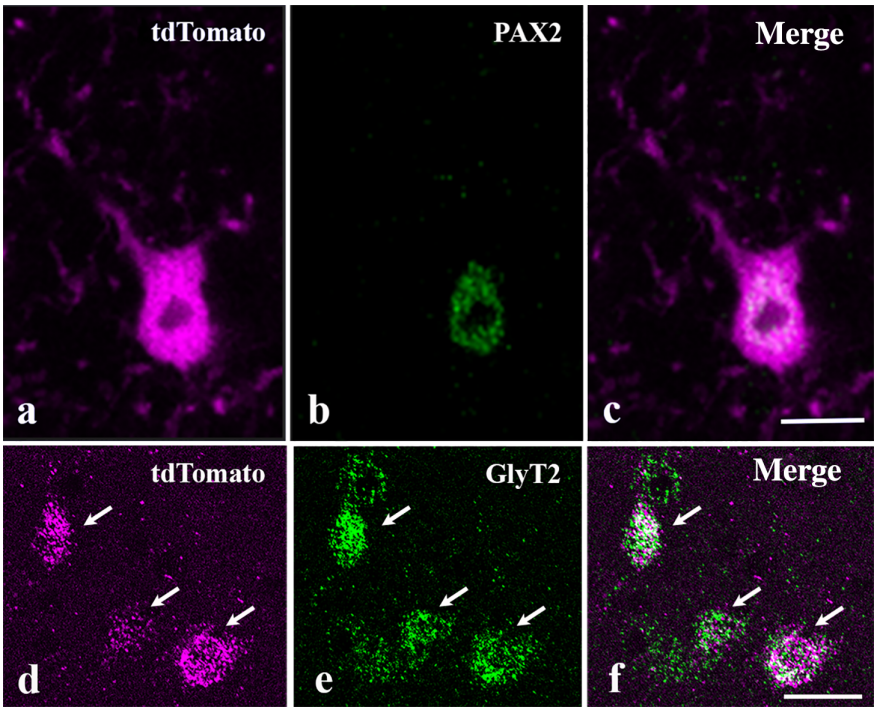

FIGURE 2 Expression of Pax2 and GlyT2 in a GlyT2::CreERT2-tdTomato-labeled neuron. (a–c) Micrograph of a single 1-μm thick confocal section obtained from a GlyT2::CreERT2-tdTomato mouse and immunostained for Pax2. The mixed color in the merged image (c) indicates the colocalization of tdTomato labeling (a; magenta) and immunostaining for Pax2 (b; green). (d, e) Micrograph of a 3-μm thick confocal section obtained from a GlyT2::CreERT2-tdTomato mouse and hybridized for tdTomato and GlyT2 mRNAs. The mixed color in the merged image (f) indicates the colocalization of tdTomato mRNA (d; magenta) and GlyT2 mRNA (e; green). Arrows on images d and e point to neurons in which tdTomato and GlyT2 mRNAs colocalize. Bars: 10 μm (a–c), 20 μm (d–f) [Color figure can be viewed at wileyonlinelibrary.com]

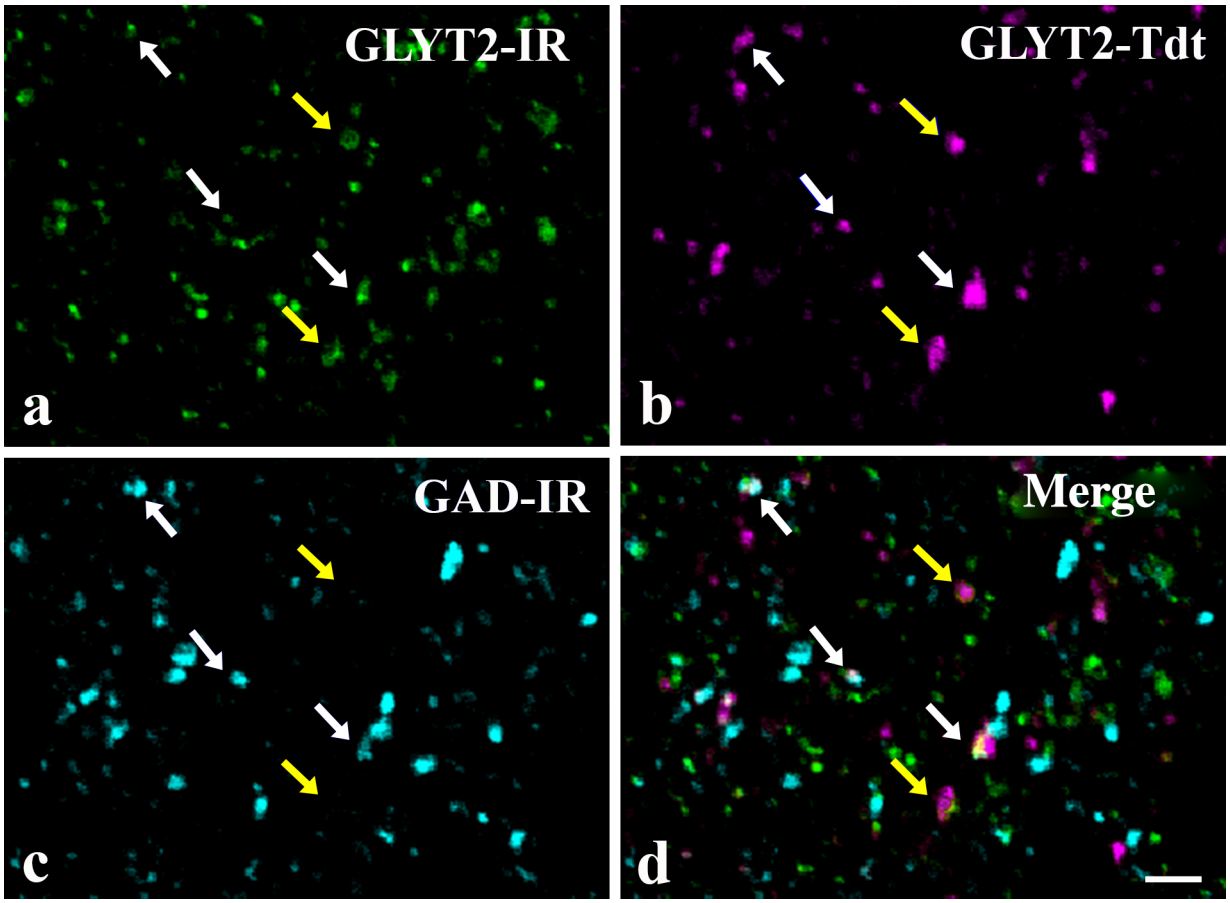

FIGURE 3 Localization of GlyT2 and GAD in GlyT2::CreERT2-tdTomato-labeled axon terminals in laminae I–II. Micrograph of a single 1-μm thick confocal section from a GlyT2::CreERT2-tdTomato mouse, which was double-immunostained for GlyT2 and GAD65/67. Large numbers of tdTomato-labeled profiles (b, magenta) show positive immunostaining for GlyT2 (a, green), and some of the tdTomato GlyT2 double-labeled puncta are also immunoreactive for GAD65/67 (c, blue). Yellow arrows point to profiles that are tdTomato labeled and immunostained for GlyT2 but negative for GAD (a-d). White arrows point to profiles that are tdTomato labeled and immunostained for both GlyT2 and GAD65/67 (a-d). Bar: 10 μm [Color figure can be viewed at wileyonlinelibrary.com]

TABLE 2 Numbers of transgenically labeled (tdTomato+) and single- (GlyT2+) as well as double-immunostained (GlyT2+ and GAD+) profiles in laminae I–II of the spinal dorsal horn

		1	2	3	4	5	6	7	8
		tdTomato+	tdTomato+ GlyT2+	2/1%	tdTomato+ GlyT2+GAD+	4/2 %	GlyT2+	GlyT2+ GAD+	7/6%
Animal 1	Section 1	17	13	76.47	6	46.15	18	10	55.55
	Section 2	20	15	75.0	6	40.0	18	7	38.88
	Section 3	15	10	66.66	5	50.0	15	6	40.0
Animal 2	Section 1	11	6	54.54	4	66.66	13	8	61.53
	Section 2	9	6	66.66	2	33.33	10	4	40.0
	Section 3	10	5	50.0	2	40.0	18	7	38.88
Animal 3	Section 1	9	5	55.55	2	40.0	11	3	27.27
	Section 2	7	5	71.42	3	60.0	11	5	45.45
	Section 3	7	3	42.85	1	33.33	9	6	66.66
Total		105	68	62.12 ± 3.94	31	45.49 ± 3.84	123	56	46.02 ± 4.22

Note: Columns 1, 2, and 4 represent the numbers when the immunostaining was observed in the tdTomato-labeled profiles. Column 3 shows the proportions of tdTomato+ profiles, which were also stained for GlyT2. Column 5 shows the proportions of tdTomato+GlyT2+ profiles, which were also stained for GAD. Columns 6 and 7 show the numbers when all GlyT2 immunostained profiles were counted, regardless, whether they were within or out of the confines of transgenically labeled profiles. Column 8 shows the proportion GlyT2+ profiles, which were also stained for GAD. The percentages in the row of "Total" represent mean values and standard error of means (*SEM*) calculated from the nine individual percentage values.

express only glycine but there are others that contain and may release both glycine and GABA.

3.3 | Morphology of GlyT2::CreERT2-tdTomato-labeled neurons

After confirming that tdTomato labels glycinergic neurons in our transgenic animals, we focused on the dendritic morphology of these neurons in laminae I–IV.

We cut transverse (X-Y plane), horizontal (X-Z plane) and sagittal (Z-Y plane) sections from the lumbar spinal cord (Figure 4). In transverse sections, we could not identify larger segments of dendritic trees of labeled neurons (Figure 4a). In horizontal sections, it became apparent that the dendrites of many tdTomato-labeled neurons show a prominent rostro-caudal orientation (Figure 4c). In addition, it turned out that although the rostro-caudal extension of the dendritic trees of these neurons was sometimes several hundred micrometer long, the medio-lateral extension of them was remarkably narrow. We have never found the medio-lateral extension of the dendritic trees wider than 50–100 μm (Figure 4c). The dendritic trees could be visualized in their largest extent in sagittal sections. In these sections, the rostro-caudal orientation of the dendritic trees appeared as nicely as in the horizontal sections, but we could also reveal that, while the dendrites were running in the rostro-caudal directions, many of them took oblique courses and extended also into the dorsal or ventral directions (Figure 4b,d). Because the dendritic arbors of the tdTomato-labeled neurons could be studied most extensively in these sections, for the investigation of the dendritic morphology of tdTomato-labeled neurons, we cut 100-μm thick sagittal sections and studied the morphology of the dendritic arbors of the labeled neurons in stacks of long series of confocal sections. In most of the cases, we were able to image and study the labeled neurons in the full 100 μm thickness of the sections. Unfortunately, the intensity of the tdTomato labeling decreased rapidly along the dendrites. Thus, it is likely that we were able to visualize only the proximal part of the dendritic trees and could not study dendrites extending further away from the cell body. In addition, although tdTomato-labeled puncta, most of which could represent axonal swellings, were densely scattered all over the investigated laminae, we were not able to identify and follow the arborization of the axons of the labeled cells. We tried to overcome this problem and intensify the tdTomato labeling with anti-tdTomato immunostaining. Although the anti-tdTomato immunostaining increased the intensity of the tdTomato signal and revealed axonal and dendritic segments within which the original tdTomato labeling was hardly visible, the antibody penetrated the sections not deeper than 10 μm. Thus, we were not able to take advantage of the immunostaining amplification of the tdTomato signal in the deep, approximately 80-μm thick layer of our 100-μm thick sections, where we collected most of our labeled neurons from.

3.3.1 | Laminae I–II

According to the shape and size of the cell bodies and dendritic morphologies, we classified tdTomato-labeled neurons in laminae I–II into three categories.

Type 1

Some cells presented small fusiform cell bodies, the short axis of which was not longer than 10 μm (Figures 5a,b and 6a). The long axis

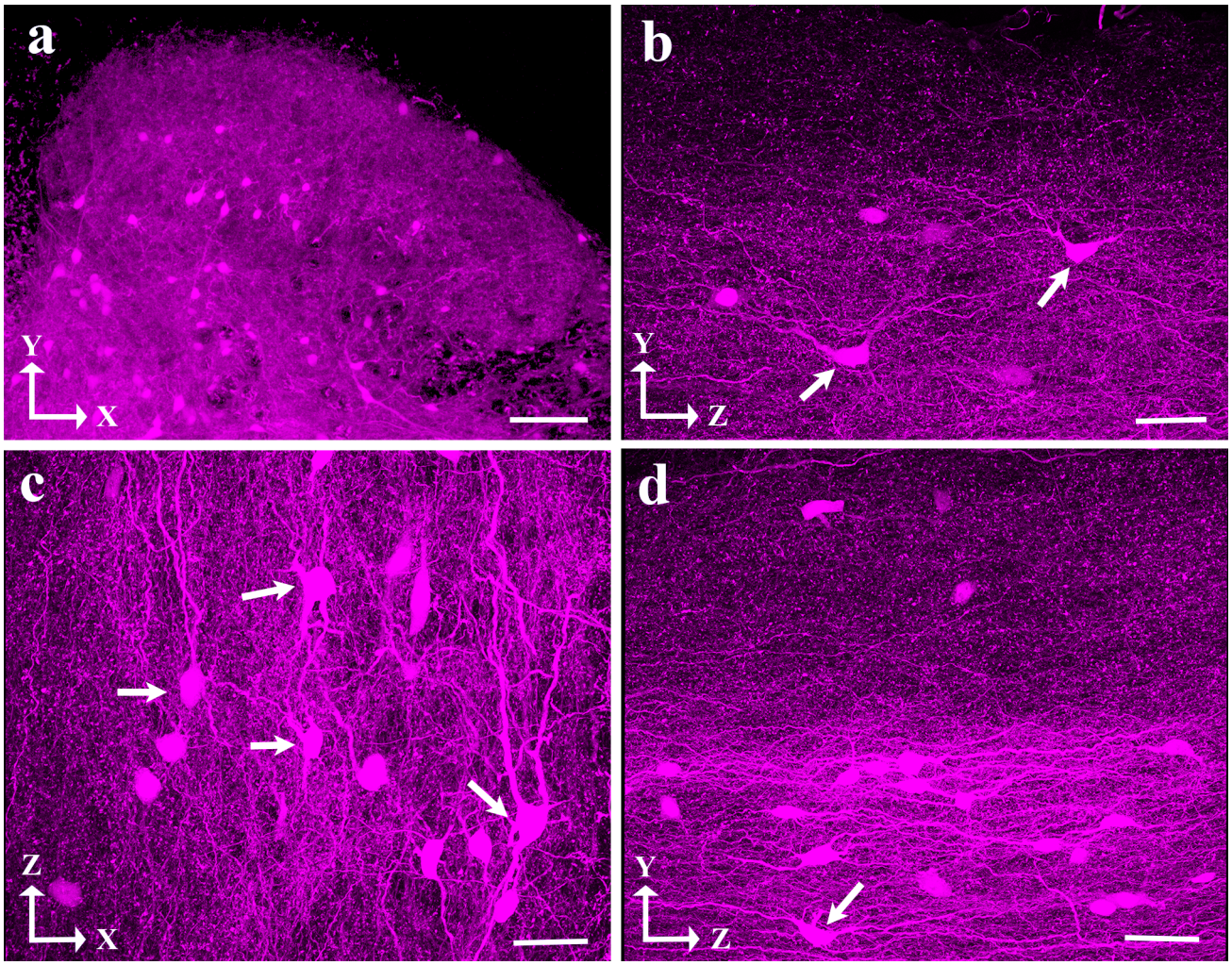

FIGURE 4 Orientation of the dendritic trees of GlyT2::CreERT2-tdTomato-labeled neurons. Micrographs showing the cell bodies, dendrites, and axons of GlyT2::CreERT2-tdTomato-labeled neurons in transverse (a), horizontal (c), and sagittal (b, d) sections of the spinal dorsal horn. The image of a horizontal section shown in c was taken approximately at the border between laminae III and IV. The upper edge of the images shown in b and d corresponds to the border between the white (dorsal funiculus) and gray (dorsal horn) matters. Note the prominent rostro-caudal orientation of the dendrites (b–d). Some of them also present a substantial dorso-ventral extension (b, d). Arrows point to cells with rostro-caudally oriented dendrites (c) and to cells the dendrites of which extend also dorsally (b, d). (Bars: 100 μm (a), 50 μm (b–d) [Color figure can be viewed at wileyonlinelibrary.com]

of the cell bodies was approximately twice as long as the short axis and was extending rostro-caudally, more or less parallel to the border between the gray and white matters. The dendrites arose from the two ends of the cell bodies and extended into the opposite rostro-caudal directions, forming a narrow, poorly arborizing dendritic tree. We were able to follow the dendrites for a distance of 40–50 μm into the rostral as well as caudal directions, whereas the dorso-ventral extension of the dendritic arbor was not wider than 20–30 μm (Figures 5a,b and 6a). In some cases, we also observed dendrites arising from the ventral aspect of the cell body (Figure 5a), but these dendrites also extended rostro-caudally, similarly to those arising from the ends of the fusiform cell body.

Type 2

Other cells presented larger, but also fusiform cell bodies. The cell bodies were approximately twice as large as those of Type 1 cells (Figures 5c and 6b). The sites of origin and the orientation of stem dendrites were similar to that of the small fusiform cells. The rostro-caudal extension of their dendrites was not longer, but the dorso-ventral extension of the dendritic arbor was wider (40–50 μm) than that of the Type 1 neurons (Figures 5c and 6b).

Type 3

Labeled cells with multipolar cell bodies and three to four stem dendrites were also observed in laminae I and IIo (Figures 5d and 6c). The diameter of the cell bodies was approximately 20 μm. Some dendrites arborized in the layer of the cell body, but most of them turned ventrally immediately after their origin form the cell body, and run obliquely for 30–40 μm distance into the ventral direction. Unfortunately, the tdTomato labeling did not allow us to follow the dendrites any longer, thus we cannot tell how far they extended ventrally.

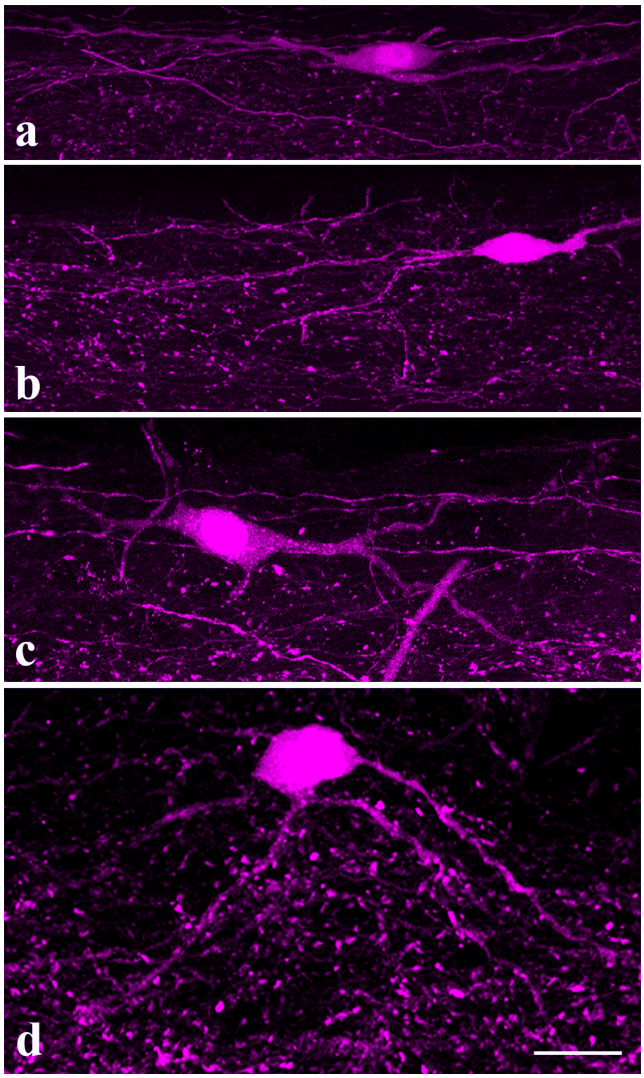

FIGURE 5 Types 1–3 of GlyT2::CreERT2-tdTomato-labeled neurons in laminae I–II of the spinal dorsal horn. The cells are illustrated in stacks of long series of confocal images (a: 55 optical sections, b: 25 optical sections, c: 95 optical sections, d: 30 optical sections) obtained from sagittal sections of the spinal cord. Bar: 20 μm [Color figure can be viewed at wileyonlinelibrary.com]

3.3.2 | Laminae III–IV

On the basis of the shape of the cell bodies and the arborization pattern of the dendritic trees, we classified the tdTomato-labeled neurons in laminae III–IV into six categories.

Type 1

Most of the cells presented small fusiform cell bodies, the shape and size of which were quite similar to those that we found also in laminae I–II (Figures 6d and 7a–d). Dendrites arose from the two poles of the cell bodies and extended rostro-caudally for at least 150 μm into both directions. The dorso-ventral extension of the dendritic tree was, however, remarkably narrow. It was rarely wider than 15–20 μm. In case of some cells, the dendrites showed a poor arborization pattern (Figure 7a,b). Other cells, however, presented dense, richly arborizing dendritic trees (Figure 7c,d).

Type 2

Some tdTomato-labeled cells presented 15–20 μm large, multipolar cell bodies with four to five stem dendrites (Figures 6e and 7f). All of the dendrites showed rich arborization and the whole dendritic tree extended rostro-caudally. The total rostro-caudal extension of the dendritic arbor was a bit shorter (200–250 μm), but the dorso-ventral expansion was wider (40–50 μm) than that of Type 1 neurons (Figures 6e and 7f).

Type 3

The size and shape of the cell bodies and the number of stem dendrites of this type of multipolar neurons resembled Type 2 cells. The arborization pattern of their dendrites was, however, remarkably different (Figures 6g and 7e). Some of the poorly arborizing dendrites extended rostro-caudally at the level of the cell bodies, others turned ventrally and formed a 50–70-μm wide dendritic tree ventral to the cell bodies (Figures 6g and 7e).

Type 4

We also observed tdTomato-labeled cells with 15–20 μm large elongated cell bodies. Typically, two dendrites arose from the two ends of the cell bodies (Figures 6f and 8b), but we also found cells that gave rise to one dendrite from one pole of the cell body but two to four dendrites from the opposite pole (Figures 6f and 8a). The dendrites presented oblique courses. While they were running into the rostral or caudal directions, they also extended dorsally. Thus, the poorly arborizing dendrites formed a dendritic arbor dorsal to the location of the cell bodies. The dendrites were running 100–150 μm into the rostral or caudal directions and extended 50–70 μm within the dorso-ventral dimension.

Type 5

A unique group of cells presented pyramidal-shaped cell bodies with three dendrites; two of them arose from the base and one from the dorsally oriented apex of the pyramid (Figures 6h and 8c,d). The two basal dendrites showed a very poor arborization and extended into the rostral and caudal directions. The 20–30-μm long initial segment of the apical dendrite run dorsally, then divided into two branches. The secondary dendritic branches changed their orientation, and while they presented further branching they took oblique orientation. This way, they approached gray matter areas located more dorsal to the cell body, and at the same time widened the dendritic field also rostro-caudally (Figures 6h and 8c,d).

Type 6

All neurons were put into this group, which did not fit to the others. For this reason, we called this type of cells as unclassified neurons. They showed certain morphological characteristics that resembled

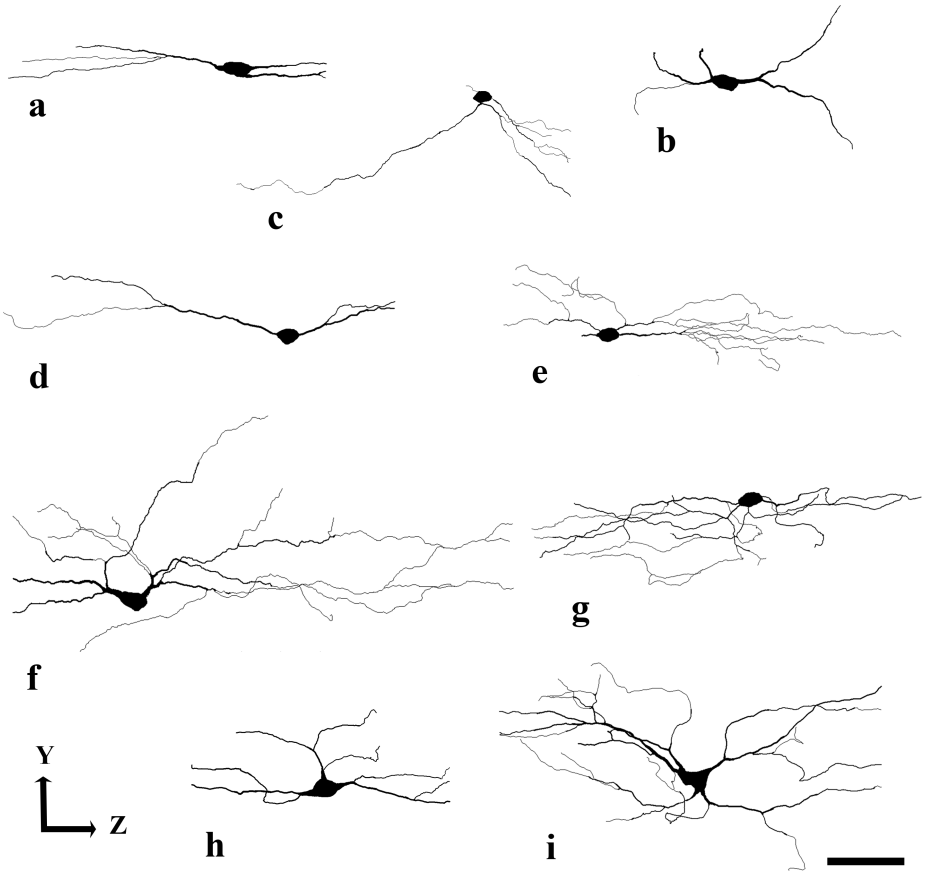

FIGURE 6 Types 1–3 and Types 1–6 of GlyT2::CreERT2-tdTomato-labeled neurons in laminae I–II and III–IV, respectively, of the spinal dorsal horn. Neurolucida drawings showing dendritic morphologies of different types of glycinergic neurons reconstructed from sagittal sections. (a) Type 1 neuron from laminae I–II, (b) Type 2 neuron from laminae I–II, (c) Type 3 neuron from laminae I–II, (d) Type 1 neuron from laminae III–IV, (e) Type 2 neuron from laminae III–IV, (f) Type 4 neuron from laminae III–IV, (g) Type 3 neuron from laminae III–IV, (h) Type 5 neuron from laminae III–IV, (i) Type 6 neuron from laminae III–IV. To estimate the laminar position of the reconstructed neurons, please identify them in Figures 5, 7, and 8 in the following way: a—Figure 5a, b—Figure 5c, c—Figure 5d, d—Figure 7b, e—Figure 7f, f—Figure 8c; g—Figure 7e, h—Figure 8c; i-Figure 8f. Bar: 50 μm

fusiform and multipolar type of neurons, but according to their dendritic arborization patterns they were different from Types 1–5 neurons, and they were different also from each other (Figures 6i and 8e,f).

3.4 | Neurochemical characterization of GlyT2::CreERT2-tdTomato-labeled neurons

Inhibitory neurons in the superficial spinal dorsal horn have been divided into five largely non-overlapping groups that had been identified by their immunoreactivity for GAL, NPY, nNOS, PV, and CR (for review, see Boyle et al., 2017; Peirs et al., 2020). It has also been reported that inhibitory neurons deeper in the dorsal horn may express the receptor tyrosine kinase Ret (RET) (Cui et al., 2016) and the nuclear orphan receptor RORβ (Del Barrio et al., 2013). Unfortunately, we were not able to find any specific and reliable antibodies against RET and RORβ. Thus, in this part of our study, we investigated GAL, NPY, nNOS, PV, and CR immunoreactivity of GlyT2::CreERT2-tdTomato-labeled neurons, whereas RET and RORβ were detected with FISH in neurons expressing tdTomato mRNA. We did not have the ambition to correlate the dendritic morphology and neurochemical character of glycinergic neurons, thus we performed this part of the experiments on transverse sections of the spinal cord. This approach gave us an opportunity to reveal GlyT2::CreERT2-tdTomato-labeled neurons within the entire medio-lateral extension of the spinal dorsal horn that resulted in the collection of lager experimental samples.

3.4.1 | Galanin and calretinin

We obtained strong cellular immunostaining for both GAL and CR in a similar laminar distribution reported earlier (Ren et al., 1993; Zhang et al., 1995). We counted 49 and 45 tdTomato-labeled cells in the areas immunostained for GAL and CR, respectively. However, we have not observed any tdTomato-labeled neurons, which were positive for these two neuronal markers.

3.4.2 | NPY

We have tested a number of anti-NPY antibodies from different vendors. Almost all of them stained NPY-containing axonal boutons heavily in laminae I–II, but none of them revealed immunostained cell bodies, although it was reported earlier (Rowan et al., 1993; Sasek & Elde, 1985). Thus, instead of studying the colocalization of NPY and tdTomato in cell bodies, we were looking for NPY immunostaining in tdTomato-labeled axon terminals. We found double-stained axon terminals only occasionally and in a remarkably low numbers (Figure 9c,g,j). Thus, our results suggest that NPY-containing cells may represent a very low proportion of glycinergic neurons.

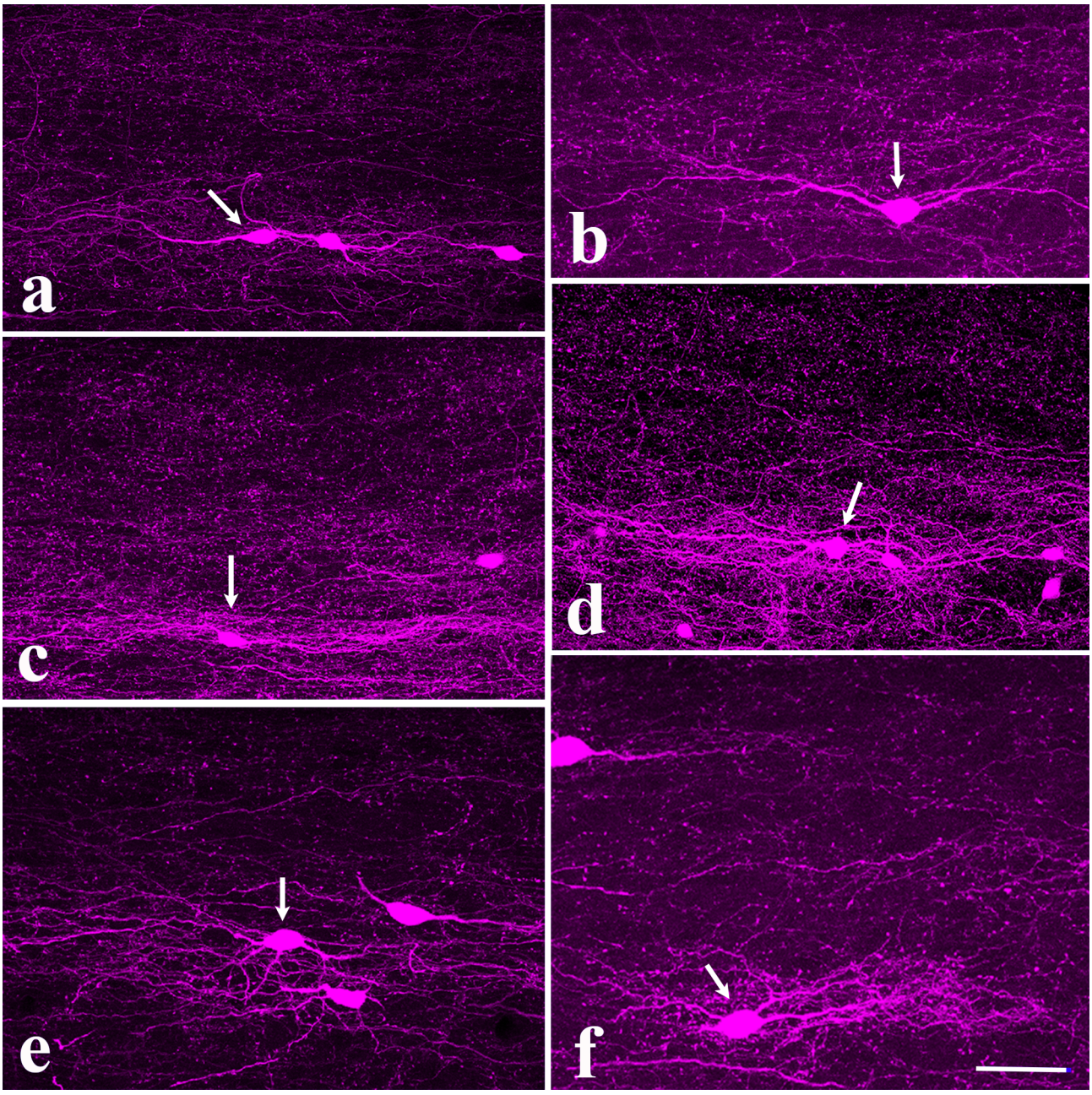

FIGURE 7 Types 1–3 of GlyT2::CreERT2-tdTomato-labeled neurons in laminae III–IV of the spinal dorsal horn. The cells are illustrated in stacks of long series of confocal images (a: 95 optical sections, b: 40 optical sections, c: 65 optical sections, d: 45 optical sections, e: 70 optical sections, f: 65 optical sections) obtained from sagittal sections of the spinal cord. Arrows point to cells of interest. Bar: 50 μm [Color figure can be viewed at wileyonlinelibrary.com]

3.4.3 | nNOS

Cell bodies were strongly immunostained for nNOS both in laminae I–II and III–IV as reported earlier (Saito et al., 1994), and some of the nNOS immunostained neurons were also labeled with tdTomato. In laminae I–II, we counted 46 tdTomato-labeled cells from which 13 (28,2%) were positive also for nNOS (Figure 9a,d,g). In laminae III–IV, 231 tdTomato-labeled neurons were found and 15 (6.5%) of them were also stained for nNOS.

3.4.4 | PV

Confirming previous results, the immunostaining for PV was very strong in the dorsal horn (Antal et al., 1990; Hughes et al., 2012; Yoshida et al., 1990). In the PV immunoreactive zone, which corresponded primarily to laminae IIi–III, but extended also into lamia IV, 367 tdTomato-labeled neurons were recovered of which 150 (40.8%) were positive for PV (Figure 9b,e,h). From the 367 neurons, 13 were found within the most superficial 60-μm thick zone of the dorsal gray matter; in the zone that

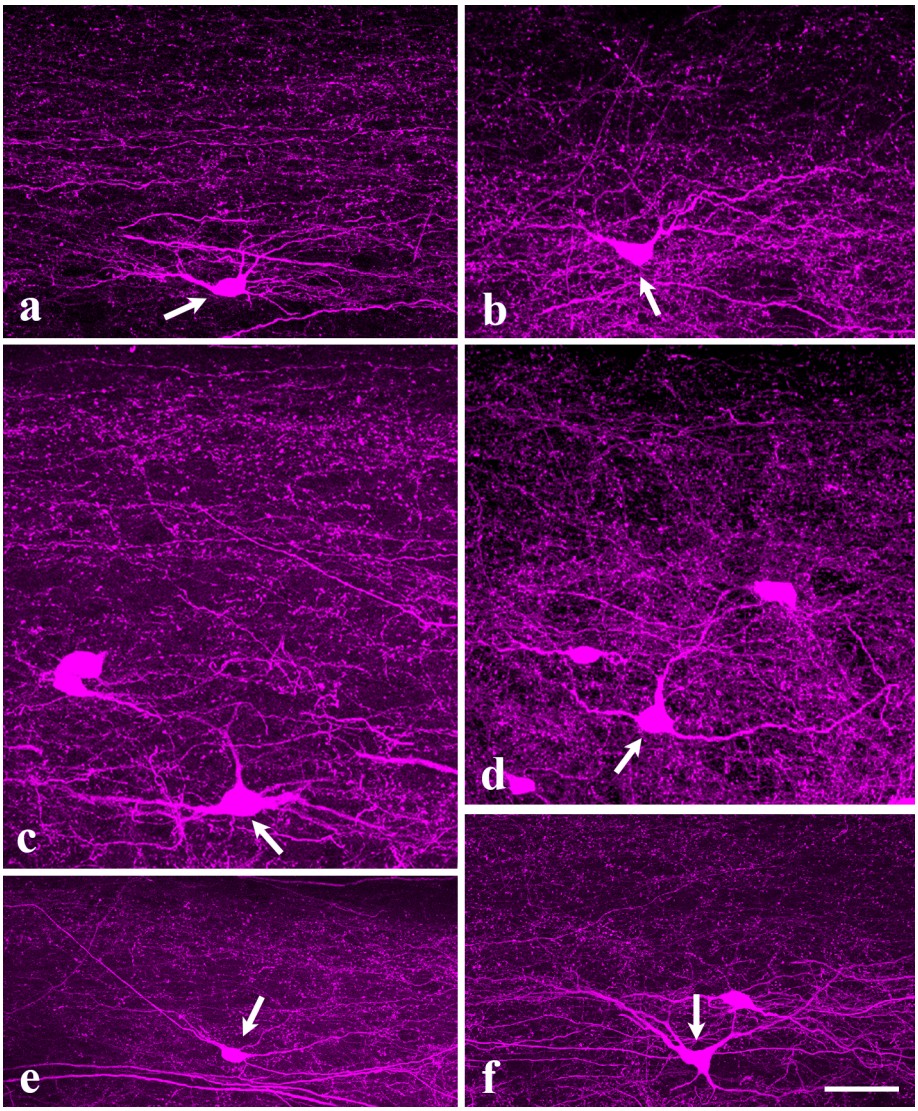

FIGURE 8 Types 4–6 of GlyT2::CreERT2-tdTomato-labeled neurons in laminae III–IV of the spinal dorsal horn. The cells are illustrated in stacks of long series of confocal images (a: 90 optical sections, b: 30 optical sections, c: 90 optical sections, d: 55 optical sections, e: 45 optical sections, f: 100 optical sections) obtained from sagittal sections of the spinal cord. Arrows point to cells of interest. Bar: 50 μm [Color figure can be viewed at wileyonlinelibrary.com]

had earlier been identified as a layer corresponding to laminae I–II in the L4–L5 segments of the mouse spinal dorsal horn (Sengul et al., 2013). Thus, these neurons can likely be regarded as cells in lamina IIi. From these 13 tdTomato-labeled neurons, six (46.1%) were positive for PV.

3.4.5 | RET

As reported earlier (Cui et al., 2016), we found many neurons in laminae III–IV, which expressed RET mRNA, but only few such neurons were present in laminae I–II. In laminae I–II, we counted 27 tdTomato-labeled cells from which 15 (55.5%) were positive also for RET. In laminae III–IV, 139 tdTomato-labeled neurons were found and 79 (56.8%) of them showed also positive hybridization signal for RET (Figure 10 d-f).

3.4.6 | RORβ

We obtained a much weaker hybridization signal for RORβ than for RET. Although the numbers of the RORβ-positive cells were much lower than that of RET-positive ones, their distribution was similar. Most of the RORβ-positive cells were found in laminae III–IV, but they were only sparsely distributed in laminae I–II, as it was reported earlier (Koch et al., 2017). We recovered 21 and 104 tdTomato-positive cells in laminae I–II and III–IV, from which 5 (23.8%) and 13 (12.5%) were positive also for RORβ, respectively (Figure 10a–c).

4 | DISCUSSION

4.1 | Specificity of the transgenic labeling of glycinergic neurons

A long line of autoradiographic, immunohistochemical, and genetic studies unequivocally confirmed that GlyT2 is exclusively expressed by glycinergic neurons and its localization is restricted to the glycine-enriched axon terminals (Luque et al., 1995; Spike et al., 1997; Poyatos 1997). This unique distribution pattern has made GlyT2 a reliable marker for glycinergic neurons. The genetic construct of the mouse line, used in this study, expressing CreERT2 recombinase

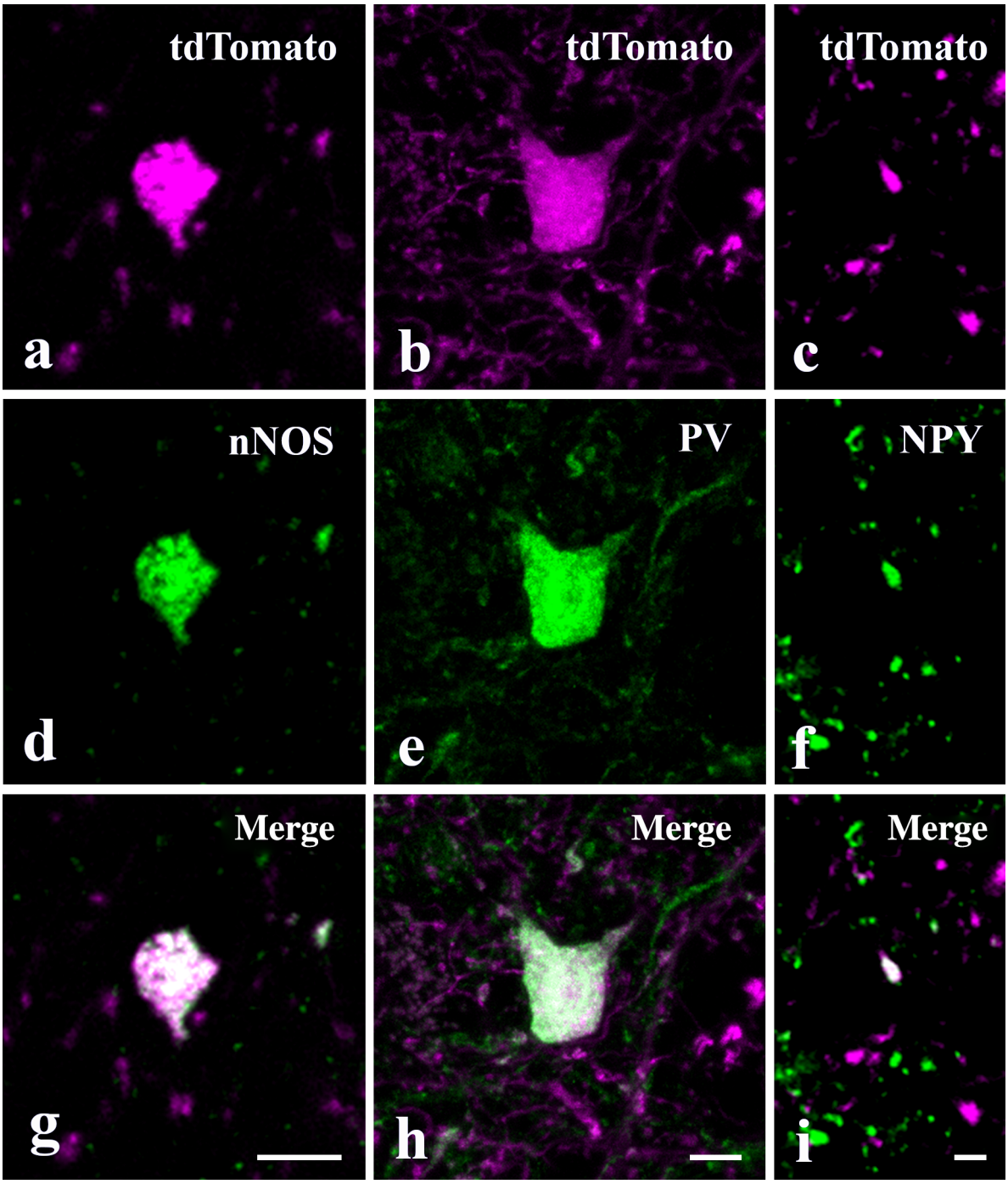

FIGURE 9 Expression of nNOS, PV, and NPY in GlyT2::CreERT2-tdTomato-labeled perikarya and axon terminal. Micrographs of a single 1-μm thick confocal section obtained from a GlyT2::Cre-tdTomato mouse and immunostained for nNOS (a, d, g), PV (b, e, h), and NPY (c, f, i). The mixed colors in the merged images (g, h, i) indicate the colocalization of tdTomato labeling (a, b, c; magenta) and positive immunostaining for nNOS (d; green), PV (e; green), and NPY (f; green). Bar: 5 μm (g, h) and 2 μm (i) [Color figure can be viewed at wileyonlinelibrary.com]

under the control of the GlyT2 gene (GlyT2::CreERT2) was generated using the same strategy previously used to generate GlyT2::Cre (Foster et al., 2015) and GlyT2::eGFP (Zeilhofer et al., 2005) animals. We crossed the GlyT2::CreERT2 animals with a tdTomato reporter line and induced tdTomato expression with intraperitoneal tamoxifen injection in the neonatal animals. The tamoxifen induction of tdTomato expression in GlyT2::CreERT2-tdTomato animals turned out to be highly specific and did not seem to be affected by transient developmental Cre expression, which was observed in case of the GlyT2::Cre-tdTomato reporter mice (Foster et al., 2015). In adult animals, virtually all, 97.35 ± 2.38% of the tdTomato-labeled cells, showed positive immunostaining for Pax2, and all of them expressed GlyT2 mRNA in the spinal dorsal horn, indicating that the tdTomato-labeled neurons were glycinergic inhibitory neurons. We have to add,

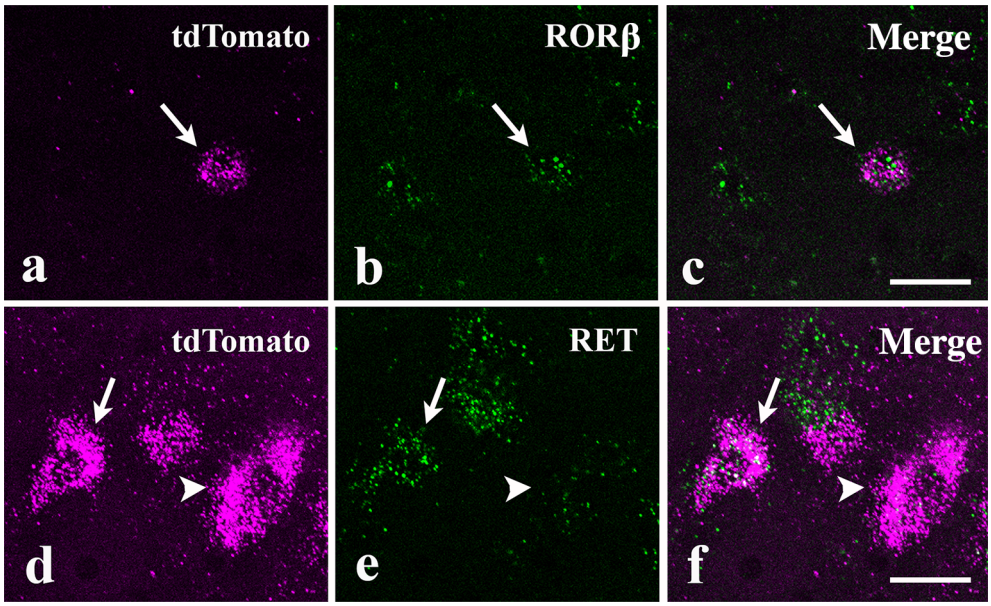

FIGURE 10 Expression of RORβ and RET mRNAs in GlyT2::CreERT2-tdTomato-labeled neurons. Micrographs of 3-μm thick confocal sections in which tdTomato (a,d), RORβ (b), and RET (e) mRNAs were detected with multiple fluorescent in situ hybridization. The mixed colors in the merged images (c, f) indicate the colocalization of tdTomato mRNA (a,d; magenta) and RORβ mRNA (b; green) as well as RET mRNA (e; green). Arrows point to neurons in which tdTomato and RORβ mRNAs (a–c) and tdTomato and RET mRNAs (d, e) colocalize. Arrowheads mark a neuron, which shows a strong hybridization signal for tdTomato and a weak one for RET. Scale bars: 20 μm [Color figure can be viewed at wileyonlinelibrary.com]

however, that with this technology we visualized only a proportion of glycinergic neurons. The number of labeled neurons depended on the age of the mice at which tamoxifen was injected. Early injections (at postnatal Days 4–5; P4–P5) resulted in high mortality, late injections (P11–P12) resulted in a moderate tdTomato expression. When injections were made on P8–P10, all injected mice survived and the resulting tdTomato labeling was satisfactorily extensive. Thus, our approach appears to be well suited for qualitative analysis of glycinergic neurons, while quantitative analyses need to be interpreted with caution.

4.2 | Glycine-only axon terminals exist in the spinal dorsal horn

It is well established that both GABA and glycine contribute to fast inhibitory transmission in the spinal dorsal horn. There are, however, contradictory results about the relative contribution of GABA- and glycine-mediated inhibition to neural events underlying spinal sensory information processing. According to some earlier studies, inhibition is primarily carried out by GABA in the superficial spinal dorsal horn, and glycine acts only as a co-transmitter in some GABAergic synapses (Todd, 1996; Todd et al., 1996). It had been shown that glycine is enriched in a proportion of GABAergic neurons, but glycine without GABA was virtually not detected in cell bodies or axon terminals in laminae I–III (Todd & Sullivan, 1990; Mitchell et al., 1993; Taal & Holstege, 1994; Todd et al., 1995, 1996; Popratiloff et al., 1996; Polgár et al., 2013). In contrast to this, others claimed that in addition to mixed GABA-glycine synaptic currents, inhibitory synaptic transmission in laminae I–III can be mediated also by GABA-only and glycine-only (Chery & de Koninck, 1999; Foster et al., 2015; Keller et al., 2001; Lu et al., 2015; Lu & Perl, 2003, 2005; Zheng et al., 2010) synaptic events in a way that neurons in laminae I–IIo receive predominantly GABAergic inputs, whereas inhibitory synaptic transmission in deeper laminae (III–IV) is dominated by glycinergic inhibition (Inquimbert et al., 2007; Takazawa et al., 2017; Takazawa & McDermott, 2010; Zeilhofer et al., 2018). To find an explanation for these contradictory observations, there is a vivid debate whether the GABA-only and glycine-only nature of synapses can be defined by pre- and/or postsynaptic mechanisms (Dugué et al., 2005; Husson et al., 2014; Muller et al., 2008). Our results substantially contribute to this debate and indicate that there are glycinergic neurons in the spinal dorsal horn that are not GABAergic, and the glycine-only nature of synapses is determined by presynaptic mechanisms. We found GAD65/67 immunostaining in only less than half of the tdTomato-labeled and GlyT2-IR axonal varicosities in laminae I–II, which indicates that there might be glycine-only inhibitory synapses in laminae I–II in a substantial number. Although our data clearly indicate the existence of glycine-only axon terminals in laminae I–II, one should take our quantitative date with necessary caution. The intensity of immunostaining for GAD65/67 in individual axon terminals varied in a wide range. There were axon terminals in which the intensity of the immunostaining signal for GAD65/67 was so weak that could hardly be recognized. In addition, it is also possible that GAD65/67 was present in such a low quantity in some axon terminals that it could not be detected with immunohistochemical methods. Thus, the actual proportions of

glycine-only axon terminals in laminae I–II can be somewhat lower than our measured values.

Because the number of tdTomato-labeled neurons was very limited in laminae I–II, it is also likely that most of these glycine-only synapses in laminae I–II are formed by axon terminals of glycinergic neurons the cell bodies of which are located in lamina III and partly in lamina IV. This notion is supported by early Golgi impregnation studies, which revealed neurons with cell bodies in lamina III and axons arborizing in lamina II (Beal et al., 1988; Maxwell et al., 1983; Réthelyi & Szentágothai, 1969). Based on their ultrastructural and degeneration studies, Réthelyi and Szentágothai (1969) suggested that the cells that they localized at the border of laminae III–IV and followed their axons into lamina II are inhibitory neurons. In the light of recent observations, one may speculate that these types of lamina III inhibitory neurons can be excited by Aβ primary afferents and project their axons to excitatory neurons in lamina II, including PKCγ- and CR-positive neurons, that are parts of neural circuits conducting Aβ primary afferent inputs to nociceptive projection neurons in lamina I (Lu et al., 2015; Peirs et al., 2021). Thus, some lamina III glycinergic neurons with axons in lamina II may play a major role in the development of allodynia (Foster et al., 2015; Lu et al., 2015; Peirs et al., 2021; Petitjean et al., 2015).

4.3 | Morphology of glycinergic neurons in laminae I–IV of the spinal dorsal horn

4.3.1 | Laminae I–II

In their early Golgi impregnation and correlative morpho-functional studies, Lima and Coimbra (1986) and Grudt and Perl (2002) presented a detailed description of neurons in lamina I and lamina II, respectively. They provided such a detailed and precise description about the morphology of these neurons that their classification proposals, especially the one of Grudt and Perl (2002) is still valid nowadays. The morphology of the tdTomato-labeled neurons that we recovered in this study also fit to these classification schemes. Our Type I and Type II cells resemble the fusiform cells of Lima and Coimbra (1986) and the islet and/or central cells of Grudt and Perl (2002). The Type 3 population of the tdTomato-labeled cells look very similar to the multipolar neurons of Lima and Coimbra (1986) and the vertical cells of Grudt and Perl (2002). Thus, according to the classification of Grudt and Perl (2002) glycinergic neurons recovered in the present study seem to be members of the islet, central, and vertical cell populations in laminae I–II. This notion is strongly reinforced by the results of Maxwell et al. (2007) and Yasaka et al. (2010) who reported that all islet cells and a proportion of central and vertical cells are inhibitory neurons.

4.3.2 | Laminae III–IV

The morphology of neurons in the deep dorsal horn is much more heterogeneous than in laminae I–II. Abraira et al. (2017) described 11 subtypes of interneurons (seven excitatory and four inhibitory) exhibiting unique morphological, physiological, and synaptic properties in the low threshold mechano-receptive zone of the dorsal horn. There is a general agreement that neurons showing very similar morphologies to those described by Grudt and Perl (2002) in laminae I–II can also be found in deeper laminae (Cui et al., 2016; Hughes et al., 2012; Koch et al., 2017), and they are among the 11 types of neurons of Abraira et al. (2017). Our present findings are in good agreement with these previous observations and notions. Our Type 1 neurons that represent most of the tdTomato-labeled cells that we found in laminae III–IV show the characteristic morphological features of islet cells (Grudt & Perl, 2002). The dendritic arborization of our Type 2 neurons is easily comparable with that of central cells (Grudt & Perl, 2002). The similarities between the morphologies of our Type 3 and Type 4 populations of neurons and of those classified as vertical cells are also obvious (Grudt and Perl, 2002). The resemblance between our Type 3 and Type 4 neurons and subpopulations of vertical neurons that were described as stalked and inverted stalked cells, respectively, in the classical Golgi impregnation studies of Gobel (1978) is even more striking. Neurons with pyramidal cell bodies (Type 5 cells in the present report) are not included in the classification of Grudt and Perl (2002), and not even mentioned in other recent publications. However, in an early Golgi impregnation study, Réthelyi and Szentágothai (1969) described pyramidal shaped neurons with cell bodies located at the border between laminae III and IV and axons projecting into lamina II. Although nobody confirmed the existence of neurons like this up till now, our present findings validate the original observation of Réthelyi and Szentágothai (1969). In accordance to the general notion that the morphology of neurons is very heterogeneous in the deep dorsal horn, we encountered a few tdTomato-labeled neurons, the dendritic arborization of which did not fit to any earlier defined cell categories and they differed even from each other (Type 6 neurons in the present article).

It is interesting to note that using a completely different experimental approach, based on the combinatorial expression of various transcription factors, Del Barrio et al. (2013) also distinguished five molecularly distinct populations of inhibitory neurons in laminae III–IV. It will be exciting to examine the correlation between inhibitory neurons defined in their study and ours.

4.4 | Neurochemical makers of glycinergic neurons in laminae I–IV of the spinal dorsal horn

4.4.1 | Laminae I–II

General consensus exists that inhibitory interneurons in laminae I–II can be divided into five populations; each of them expressing one of the following markers: GAL, NPY, nNOS, PV, and CR (Boyle et al., 2017). It should be noted, however, that this classification was made based on the assumption that virtually all inhibitory neurons were GABAergic in laminae I–II. Thus, the expression of the five markers was investigated in neurons that were identified as

GABAergic (Duan et al., 2014; Polgár et al., 2013; Sardella et al., 2011, b; Tiong et al., 2011).

Our present results, on one hand, partly confirm this idea and suggest that some of the nNOS- and PV-containing GABAergic neurons in laminae I–II and lamina IIi, respectively, also express glycine. However, we did not find any GAL and CR, and only minimal, if any, NPY expression in the tdTomato-labeled glycinergic neurons. Thus, we conclude that glycine colocalizes with GABA in some nNOS- and PV-positive GABAergic neurons, but the GAL, CR, and most of the NPY expressing inhibitory neurons are likely to be GABA-only cells.

On the other hand, we did not find nNOS and PV staining in more than two-thirds and about one-fourth of the tdTomato-labeled glycinergic neurons in laminae I–IIo, and lamina IIi, respectively. First in the literature, this observation clearly suggests that glycinergic neurons cannot be regarded simply as a subpopulation of GABAergic neurons in laminae I–II. Although they are present in low numbers, at least two-thirds and one-fourth of glycinergic cells in laminae I–IIo and lamina IIi, respectively, are glycine-only neurons, which do not express the markers that were used for the identification of GABAergic cells. Our data also indicate, most, if not all, of these glycine-only neurons express RORβ and/or RET.

4.4.2 | Laminae III–IV

There is general agreement that inhibitory interneurons in laminae III–IV are much more heterogeneous than those in laminae I–II. Although it has been shown that PV and nNOS are also expressed by some inhibitory neurons in laminae III and IV (Tiong et al., 2011; Polgár et al. 2013), these laminae contain much larger populations of inhibitory neurons expressing RET (Cui et al., 2016) and RORβ (Koch et al., 2017). In addition, there are many other inhibitory neurons that cannot be identified by one single neurochemical marker, but only by clustering of various factors obtained by single-cell transcriptomic analysis (Häring et al., 2018; Sathyamurthy et al., 2018; Zeisel et al., 2018).

Our present results are consistent with earlier studies on the neurochemical characterization of glycinergic neurons in laminae III–IV. An important new finding of the present work is that in laminae III–IV approximately 56, 40, 12, and 6% of the tdTomato-labeled glycinergic neurons were RET, PV, RORβ, and nNOS positive, respectively. Thus, although the degree of colocalization of PV, RORβ, and RET is unknown, our data indicate that most of the glycinergic neurons co-express PV, RORβ, or RET. Some of them also express nNOS, and it is also possible that there are other smaller neurochemical populations that are still awaiting proper neurochemical identification.

ACKNOWLEDGMENTS

This work was supported by the Hungarian Academy of Sciences (MTA-TKI 242) and the Hungarian National Brain Research Program (KTIA_NAP_13-1-2013-0001) to MA, and by the Swiss National Science Foundation (SNSF; grant number 310030_197888) to HUZ.

CONFLICT OF INTEREST

The authors have no financial and non-financial conflict of interest to declare.

PEER REVIEW

The peer review history for this article is available at https://publons.com/publon/10.1002/cne.25232.

DATA AVAILABILITY STATEMENT

The data that support the findings of this study are available from the corresponding author upon reasonable request.

ORCID

Miklós Antal https://orcid.org/0000-0002-2457-7387

REFERENCES

Abraira, V. E., Kuehn, E. D., Chirila, A. M., Springel, M. W., Toliver, A. A., Zimmerman, A. L., Orefice, L. L., Boyle, K. A., Bai, L., Song, B. J., Bashista, K. A., O'Neill, T. G., Zhuo, J., Tsan, C., Hoynoski, J., Rutlin, M., Kus, L., Niederkofler, V., Watanabe, M., Dymecki, S. M., Nelson, S. B., Heintz, N., Hughes, D.I., & Ginty, D. D. (2017). The cellular and synaptic architecture of the mechanosensory dorsal horn. *Cell*, *168*, 295–310. https://doi.org/10.1016/j.cell.2016.12.010

Alaynick, W. A., Jessell, T. M., & Pfaff, S. A. (2011). Snapshot: Spinal cord development. *Cell*, *146*, 178. https://doi.org/10.1016/j.cell.2011.06.038

Antal, M., Freund, F. F., & Polgár, E. (1990). Calcium-binding proteins, parvalbumin- and calbindin-D 28k-immunoreactive neurons in the rat spinal cord and dorsal root ganglia: A light and electron microscopic study. *The Journal of Comparative Neurology*, *295*, 467–484. https://doi.org/10.1002/cne.902950310

Aubrey, K. R., & Supplisson, S. (2018). Heterogeneous signaling at GABA and glycine co-releasing terminal. *Frontiers in Synaptic Neuroscience*, *10*, 40.

Augustine, V., Gokce, S. K., Lee, S., Wang, B., Davidson, T. J., Reimann, F., Gribble, F., Deisseroth, K., Lois, C., & Oka, Y. (2018). Hierarchical neural architecture underlying thirst regulation. *Nature*, *555*, 204–209. https://doi.org/10.1038/nature25488

Balázs, A., Mészár, Z., Hegedűs, K., Kenyeres, A., Hegyi, Z., Dócs, K., & Antal, M. (2017). Development of putative inhibitory neurons in the embryonic and postnatal mouse superficial spinal dorsal horn. *Brain Structure and Function*, *222*, 2157–2171. https://doi.org/10.1007/s00429-016-1331-9

Beal, J. A., Russell, C. T., & Knight, D. S. (1988). Morphological and developmental characterization of local-circuit neurons in lamina III of the rat spinal cord. *Neuroscience Letters*, *86*, 1–5. https://doi.org/10.1016/0304-3940(88)90172-3

Boyle, K. A., Gutierrez-Mecinas, M., Polgar, E., Mooney, N., O'Connor, E., Furuta, T., Watanabe, M., & Todd, A. J. (2017). A quantitative study of neurochemically defined populations of inhibitory interneurons in the superficial dorsal horn of the mouse spinal cord. *Neuroscience*, *363*, 120–133. https://doi.org/10.1016/j.neuroscience.2017.08.044

Celio, M. R., Baier, W., Schärer, L., de Viragh, P. A. & Gerday, C. (1988). Monoclonal antibodies directed against the calcium binding protein parvalbumin. *Cell Calcium*, *9*, 81–86. https://doi.org/10.1016/0143-4160(88)90027-9

Chery, N., & de Koninck, Y. (1999). Junctional versus extrajunctional glycine and GABA(A) receptor-mediated IPSCs in identified lamina I neurons of the adult rat spinal cord. *The Journal of Neuroscience*, *19*,

7342–7355. https://doi.org/10.1523/JNEUROSCI.19-17-07342.1999

Corleto, J. A., Bravo-Hernandez, M., Kamizato, K., Kakinihana, O., Santucci, C., Navarro, M. R., Platoshyn, O., Cizkova, D., Lukacova, N., Taylor, J., & Marsala, M. (2015). Thoracic 9 spinal transection-induced model of muscle spasticity in the rat: A systematic electrophysiological and histopathological characterization. *PLoS One*, *10*, e0144642. https://doi.org/10.1371/journal.pone.0144642

Cui, L., Miao, X., Liang, L., Abdus-Saboor, I., Olson, W., Fleming, M. S., Ma, M., Tao, Y. X., & Luo, W. (2016). Identification of early RET+ deep dorsal spinal cord interneurons in gating pain. *Neuron*, *91*, 1137–1153. https://doi.org/10.1016/j.neuron.2016.07.038

Del Barrio, M. G., Bourane, S., Grossmann, K., Schüle, R., Britsch, S., O'Leary, D. D. M., & Goulding, M. (2013). A transcription factor code defines nine sensory interneuron subtypes in the mechanosensory area of the spinal cord. *PLoS One*, *8*, e77928. https://doi.org/10.1371/journal.pone.0077928

Dressler, G. R., & Doughlass, E. C. (1992). Pax-2 is a DNA-binding protein expressed in embryonic kidney and Wilms tumor. *Proceedings of the National Academy of Sciences of the United States of America*, *89*, 1179–1183. https://doi.org/10.1073/pnas.89.4.1179

Duan, B., Cheng, L., Bourane, S., Britz, O., Padilla, C., Garcia-Campmany, L., Krashes, M., Knowlton, W., Velasquez, T., Ren, X., Ross, S., Lowell, B. B., Wang, Y., Martyn Goulding, M., & Ma, Q. (2014). Identification of spinal circuits transmitting and gating mechanical pain. *Cell*, *159*, 1417–1432. https://doi.org/10.1016/j.cell.2014.11.003

Dugué, G. P., Dumoulin, A., Triller, A., & Dieudonné, S. (2005). Target-dependent use of coreleased inhibitory transmitters at central synapses. *Journal of Neuroscience*, *25*, 6490–6498. https://doi.org/10.1523/JNEUROSCI-1500-05.2005

Filice, F., Celio, M. R., Babalian, A., Blum, W., & Szabolcsi, V. (2017). Parvalbumin-expressing ependymal cells in rostral lateral ventricle wall adhesions contribute to aging-related ventricle stenosis in mice. *The Journal of Comparative Neurology*, *525*, 3266–3285. https://doi.org/10.1002/cne.24276

Foster, E., Wildner, H., Tudeau, L., Haueter, S., Ralvenius, W. T., Jegen, M., Johanssen, H., Hösli, L., Haenraets, K., Ghanem, A., Conzelmann, K. K., Bösl, M., & Zeilhofer, H. U. (2015). Targeted ablation, silencing, and activation establish glycinergic dorsal horn neurons as key components of a spinal gate for pain and itch. *Neuron*, *85*, 1289–1304. https://doi.org/10.1016/j.neuron.2015.02.028

Glavas, M. M., Grayson, B. E., Allen, S. E., Copp, D. R., Smith, M. S., Cowley, M. A., & Grove, K. L. (2008). Characterization of brainstem peptide YY (PYY) neurons. *The Journal of Comparative Neurology*, *506*, 194–210. https://doi.org/10.1002/cne.21543

Gobel, S. (1978). Golgi studies of the neurons in layer I of the dorsal horn of the medulla (trigeminal nucleus caudalis). *The Journal of Comparative Neurology*, *180*, 375–394. https://doi.org/10.1002/cne.901800213

Grudt, T. J., & Perl, E. R. (2002). Correlations between neuronal morphology and electrophysiological features in the rodent superficial dorsal horn. *The Journal of Physiology*, *540*, 189–207. https://doi.org/10.1113/jphysiol.2001.012890

Häring, M., Zeisel, A., Hochgerner, H., Rinwa, P., Jakobsson, J. E. T., Lönnerberg, P., La Manno, G., Sharma, N., Borgius, L., Kiehn, O., Lagerström, M. C., Linnarsson, S., & Ernfors, P. (2018). Neuronal atlas of the dorsal horn defines its architecture and links sensory input to transcriptional cell types. *Nature Neuroscience*, *21*, 869–880. https://doi.org/10.1038/s41593-018-0141-1

Hughes, D. I., Sikander, S., Kinnon, C. M., Boyle, K. A., Watanabe, M., Callister, R. J., & Graham, B. A. (2012). Morphological, neurochemical and electrophysiological features of parvalbumin-expressing cells: A likely source of axo-axonic inputs in the mouse spinal dorsal horn. *The Journal of Physiology*, *590*, 3927–3951. https://doi.org/10.1113/jphysiol.2012.235655

Husson, Z., Rousseau, C. V., Broll, I., Hanns Ulrich Zeilhofer, H. U., & Dieudonné, S. (2014). Differential GABAergic and glycinergic inputs of inhibitory interneurons and Purkinje cells to principal cells of the cerebellar nuclei. *Journal of Neuroscience*, *34*, 9418–9431. 10.1523/JNEUROSCI

Ikegami, I., Shimizu, I., Sato, T., Yoshida, Y., Hayashi, Y., Suda, M., Katsuumi, G., Li, J., Wakasugi, T., Minokoshi, Y., Okamoto, S., Hinoi, E., Nielsen, S., Jespersen, Z. N., Scheele, C., Soga, T., & Minamino, T. (2018). Gamma-aminobutyric acid signaling in brown adipose tissue promotes systemic metabolic derangement in obesity. *Cell Reports*, *24*, 2827–2837. https://doi.org/10.1016/j.celrep.2018.08.024

Ikenaga, T., Urban, J. M., Gebhart, N., Hatta, K., Kawakami, K., & Ono, F. (2011). Formation of the spinal network in zebrafish determined by domain-specific Pax genes. *The Journal of Comparative Neurology*, *519*, 1562–1579. https://doi.org/10.1002/cne.22585

Inquimbert, P., Rodeau, J. L., & Schlichter, R. (2007). Differential contribution of GABAergic and glycinergic components to inhibitory synaptic transmission in lamina II and laminae III-IV of the young rat spinal cord. *The European Journal of Neuroscience*, *26*, 2940–2949. https://doi.org/10.1111/j.1460-9568.2007.05919.x

Keller, A. F., Coull, J. A., Chery, N., Poisbeau, P., & de Koninck, Y. (2001). Region-specific developmental specialization of GABA-glycine cosynapses in laminas I-II of the rat spinal dorsal horn. *The Journal of Neuroscience*, *21*, 7871–7880. https://doi.org/10.1523/JNEUROSCI.21-20-07871.2001

Kim, E. J., Hori, K., Wyckoff, A., Dickel, L. K., Koundakjian, E. J., Goodrich, L. V., & Johnson, J. E. (2011). Spatiotemporal fate map of neurogenin1 (Neureg1) lineages in the mousecentral nervous system. *The Journal of Comparative Neurology*, *519*, 1355–1370. https://doi.org/10.1002/cne.22574

Koch, S. C., Acton, D., & Goulding, M. (2018). Spinal circuits for touch, pain, and itch. *Annual Review of Physiology*, *80*, 189–217. https://doi.org/10.1146/annurev-physiol-022516-034303

Koch, S. C., Del Barrio, M. G., Dalet, A., Gatto, G., Günther, T., Zhang, J., Seidler, B., Saur, D., Schüle, R., & Goulding, M. (2017). RORβ spinal interneurons gate sensory transmission during locomotion to secure a fluid walking gate. *Neuron*, *96*, 1419–1431. https://doi.org/10.1016/j.neuron.2017.11.011

Landry, M., Bouali-Benazzouz, R., Andre, C., Shi, T. J. S., Leger, C., Nagy, F., & Hökfelt, T. (2006). Galanin receptor 1 is expressed in a subpopulation of glutamatergic interneurons in the dorsal horn of the rat spinal cord. *The Journal of Comparative Neurology*, *499*, 391–403. https://doi.org/10.1002/cne.21109

Lima, D., & Coimbra, A. (1986). A Golgi study of the neuronal population of the marginal zone (lamina I) of the rat spinal cord. *The Journal of Comparative Neurology*, *244*, 53–71. https://doi.org/10.1002/cne.902440105

Lu, Y., Dong, H., Gao, Y., Gong, Y., Ren, Y., Gu, N., Zhou, S., Xia, N., Sun, Y. Y., Ji, R. R., & Xiong, L. (2015). A feed-forward spinal cord glycinergic neural circuit gates mechanical allodynia. *The Journal of Clinical Investigation*, *123*, 4050–4062. https://doi.org/10.1172/JCI70026

Lu, Y., & Perl, E. R. (2003). A specific inhibitory pathway between substantia gelatinosa neurons receiving direct C-fiber input. *The Journal of Neuroscience*, *23*, 8752–8758. https://doi.org/10.1523/JNEUROSCI.23-25-08752.2003

Lu, Y., & Perl, E. R. (2005). Modular organization of excitatory circuits between neurons of the spinal superficial dorsal horn (laminae I and II). *The Journal of Neuroscience*, *25*, 3900–3907. https://doi.org/10.1523/JNEUROSCI.0102-05.2005

Luque, J. M., Nelson, N., & Richards, J. G. (1995). Cellular expression of glycine transporter 2 messenger RNA exclusively in rat hindbrain and spinal cord. *Neuroscience*, *64*, 525–535. https://doi.org/10.1016/0306-4522(94)00404-s

Maxwell, D. J., Belle, M. D., Cheunsuang, O., Stewart, A., & Morris, R. (2007). Morphology of inhibitory and excitatory interneurons in superficial laminae of the rat dorsal horn. *The Journal of Physiology*, *584*, 521–533. https://doi.org/10.1113/jphysiol.2007.140996

Maxwell, D. J., Fyffe, R. E. W., & Réthelyi, M. (1983). Morphological properties of physiologically characterized lamina III neurons in the cat spinal cord. *Neuroscience*, *10*, 1–22. https://doi.org/10.1016/0306-4522(83)90076-3

McClung, J. R., & Castro, A. J. (1978). Rexed's laminae as it applies to the rat cervical spinal cord. *Experimental Neurology*, *58*, 145–148.

McNeil, D. L., Chung, K., Hulsebosch, C. E., Bolander, R. P., & Coggeshall, R. E. (1988). Numbers of synapses in laminae I-IV of the rat dorsal horn. *The Journal of Comparative Neurology*, *278*, 453–460. https://doi.org/10.1002/cne.902780313

Mitchell, K., Spike, R. C., & Todd, A. J. (1993). An immunocytochemical study of glycine receptor and GABA in laminae I-III of rat spinal dorsal horn. *The Journal of Neuroscience*, *13*, 2371–2381. https://doi.org/10.1523/JNEUROSCI.13-06-02371.1993

Molander, C., Xa, Q., & Grant, G. (1984). The cytoarchitectonic organization of the spinal cord in the rat. I. The lower thoracic and lumbosacral cord. *Journal of Comparative Neurology*, *230*, 133–141. https://doi.org/10.1002/cne.902300112

Muller, E., Le-Corronc, H., & Legendre, P. (2008). Extrasynaptic and postsynaptic receptors in glycinergic and GABAergic neurotransmission: A division of labor? *Frontiers in Molecular Neuroscience*, *1*, 3. https://doi.org/10.3389/neuro.02.003

Peirs, C., Dallel, R., & Todd, A. J. (2020). Recent advances in our understanding of the organization of dorsal horn neuron populations and their contribution to cutaneous mechanical allodynia. *Journal of Neural Transmission*, *127*, 505–525. https://doi.org/10.1007/s00702-020-02159-1

Peirs, C., & Seal, R. P. (2016). Neural circuits for pain: Recent advances and current views. *Science*, *354*, 578–584. https://doi.org/10.1126/science.aaf8933

Peirs, C., Williams, S. G., Zhao, X., Arokiaraj, C. M., Ferreira, D. W., Noh, M. C., Smith, K. M., Halder, P., Corrigan, K. A., Gedeon, J. Y., Lee, S. J., Gatto, G., Chi, D., Ross, S. E., Goulding, M., & Seal, R. P. (2021). Mechanical allodynia circuitry in the dorsal horn is defined by the nature of the injury. *Neuron*, *109*, 73–90.e7. https://doi.org/10.1016/j.neuron.2020.10.027

Petitjean, H., Pawlowski, S. A., Fraine, S. L., Sharif, B., Hamad, D., Fatima, T., Berg, J., Brown, C. M., Jan, L. Y., Ribeiro-da-Silva, A., Braz, J. M., Basbaum, A. I., & Sharif-Naeini, R. (2015). Dorsal horn parvalbumin neurons are gate-keepers of touch-evoked pain after nerve injury. *Cell Reports*, *13*, 1246–1257. https://doi.org/10.1016/j.celrep.2015.09.080

Polgár, E., Durrieux, C., Hughes, D. I., & Todd, A. J. (2013). A quantitative study of inhibitory interneurons in laminae I-III of the mouse spinal dorsal horn. *PLoS One*, *8*, e78309. https://doi.org/10.1371/journal.pone.0078309

Polgar, E., Sardella, T. C. P., Watanabe, M., & Todd, A. J. (2011). Quantitative study of NPY-expressing GABAergic neurons and axons in rat spinal dorsal horn. *The Journal of Comparative Neurology*, *519*, 1007–1023. https://doi.org/10.1002/cne.22570

Popratiloff, A., Valtschanoff, J. G., Rustioni, A., & Weinberg, R. J. (1996). Co-localization of GABA and glycine in the rat dorsal column nuclei. *Brain Research*, *706*, 308–312. https://doi.org/10.1016/0006-8993(95)01280-x

Powell, J. J., & Todd, A. J. (1992). Light and electron microscope study of GABA-immunoreactive neurones in lamina III of rat spinal cord. *The Journal of Comparative Neurology*, *315*, 125–136. https://doi.org/10.1002/cne.903150202

Poyatos, I., Ponce, J., Aragón, C., Giménez, C., & Zafra, F. (1997). The glycine transporter GLYT2 is a reliable marker for glycine-immunoreactive neurons. *Brain Research. Molecular Brain Research*, *49*, 63–70. https://doi.org/10.1016/s0169-328x(97)00124-1

Punnakkal, P., Schoultz, C., Haenraets, K., Wildner, H., & Zeilhofer, H. U. (2014). Morphological, biophysical and synaptic properties of glutamatergic neurons of the mouse spinal dorsal horn. *The Journal of Physiology*, *592*, 759–776. https://doi.org/10.1113/jphysiol.2013.264937

Ren, K., Ruda, M. A., & Jacobowitz, D. M. (1993). Immunohistochemical localization of calretinin in the dorsal root ganglion and spinal cord of the rat. *Brain Research Bulletin*, *31*, 13–22. https://doi.org/10.1016/0361-9230(93)90004-U

Réthelyi, M., & Szentágothai, J. (1969). The large synaptic complexes of the substantia gelatinosa. *Experimental Brain Research*, *7*, 258–274. https://doi.org/10.1007/BF00239033

Rowan, S., Todd, A. J., & Spike, R. C. (1993). Evidence that neuropeptide Y is present in GABAergic neurons in the superficial dorsal horn of the rat spinal cord. *Neuroscience*, *53*, 537–545. https://doi.org/10.1016/0306-4522(93)90218-5

Saito, S., Kidd, G. J., Trapp, B. D., Dawson, T. M., Bredt, D. S., Wilson, D. A., Traystman, R. J., Snyder, S. H., & Hanley, D. F. (1994). Rat spinal cord neurons contain nitric oxide synthase. *Neuroscience*, *59*, 447–456. https://doi.org/10.1016/0306-4522(94)90608-4

Sardella, T. C. P., Polgár, E., Garzillo, F., Furuta, T., Kaneko, T., Watanabe, M., & Todd, A. J. (2011). Dynorphin is expressed primarily by GABAergic neurons that contain galanin in the rat dorsal horn. *Molecular Pain*, *7*, 76. https://doi.org/10.1186/1744-8069-7-76

Sardella, T. C. P., Polgár, E., Watanabe, M., & Todd, A. J. (2011). A quantitative study of neuronal nitric oxide synthase expression in laminae I-III of the rat spinal dorsal horn. *Neuroscience*, *192*, 708–720. https://doi.org/10.1016/j.neuroscience.2011.07.011

Sasek, C. A., & Elde, R. P. (1985). Distribution of neuropeptide Y-like immunoreactivity and its relationship to FMRF-amide-like immunoreactivity in the sixth lumbar and first sacral spinal cord segments of the rat. *The Journal of Neuroscience*, *5*, 1729–1739. https://doi.org/10.1523/JNEUROSCI.05-07-01729.1985

Sathyamurthy, A., Johnson, K. R., Matson, K. J. E., Dobrott, C. I., Li, L., Ryba, A. R., Bergman, T. B., Kelly, M. C., Kelley, M. W., & Levine, A. J. (2018). Massively parallel single nucleus transcriptional profiling defines spinal cord neurons and their activity during behavior. *Cell Reports*, *22*, 2216–2225. https://doi.org/10.1016/j.celrep.2018.02.003

Sengul, G., Watson, C., Tanaka, I., & Paxinos, G. (2013). *Atlas of the spinal cord of the rat, mouse, marmoset, rhesus, and human*. Elsevier.

Simmons, D. R., Spike, R. C., & Todd, A. J. (1995). Galanin is contained in GABAergic neurons in the rat spinal dorsal horn. *Neuroscience Letters*, *187*, 119–122. https://doi.org/10.1016/0304-3940(95)11358-4

Smith, K. M., Boyle, K. A., Madden, J. F., Dickinson, S. A., Jobling, P., Callister, R. J., Hughes, D. I., & Graham, B. A. (2015). Functional heterogeneity of calretinin-expressing neurons in the mouse superficial dorsal horn: Implications for spinal pain processing. *The Journal of Physiology*, *593*, 4319–4339. https://doi.org/10.1113/JP270855

Spike, R. C., Watt, C., Zafra, F., & Todd, A. J. (1997). An ultrastructural study of the glycine transporter GLYT2 and its association with glycine in the superficial laminae of the rat spinal dorsal horn. *Neuroscience*, *77*, 543–551. https://doi.org/10.1016/s0306-4522(96)00501-5

Taal, W., & Holstege, J. C. (1994). GABA and glycine frequently colocalize in terminals on cat spinal motoneurons. *Neuroreport*, *5*, 2225–2228. https://doi.org/10.1097/00001756-199411000-00005

Takazawa, T., Choudhury, P., Tong, C. K., Conway, C. M., Scherrer, G., Flood, P. D., Mukai, J., & MacDermott, A. B. (2017). Inhibition mediated by glycinergic and GABAergic receptors on excitatory neurons in mouse superficial dorsal horn is location-specific but modified by inflammation. *The Journal of Neuroscience*, *37*, 2336–2348. https://doi.org/10.1523/JNEUROSCI.2354-16.2017

Takazawa, T., & McDermott, A. B. (2010). Glycinergic and GABAergic tonic inhibition fine tune inhibitory control in regionally distinct

subpopulations of dorsal horn neurons. *The Journal of Physiology*, *588*, 2571–2587. https://doi.org/10.1113/jphysiol.2010.188292

Tiong, S. Y. X., Polgár, E., van Kralingen, J. C., Watanabe, M., & Todd, A. J. (2011). Galanin-immunoreactivity identifies a distinct population of inhibitory interneurons in laminae I-III of the rat spinal cord. *Molecular Pain*, *7*, 36. https://doi.org/10.1186/1744-8069-7-36

Todd, A. J. (1996). GABA and glycine in synaptic glomeruli of the rat spinal dorsal horn. *The European Journal of Neuroscience*, *8*, 2492–2498. https://doi.org/10.1111/j.1460-9568.1996.tb01543.x

Todd, A. J., Spike, R. C., Chong, D., & Neilson, M. (1995). The relationship between glycine and gephyrin in synapses of the rat spinal cord. *The European Journal of Neuroscience*, *7*, 1–11. https://doi.org/10.1111/j.1460-9568.1995.tb01014.x

Todd, A. J., & Sullivan, A. C. (1990). Light microscope study of the coexistence of GABA-like and glycine-like immunoreactivities in the spinal cord of the rat. *The Journal of Comparative Neurology*, *296*, 496–505. https://doi.org/10.1002/cne.902960312

Todd, A. J., Watt, C., Spike, R. C., & Sieghart, W. (1996). Co-localization of GABA, glycine, and their receptors at synapses in the rat spinal cord. *The Journal of Neuroscience*, *16*, 974–982. https://doi.org/10.1523/JNEUROSCI.16-03-00974.1996

Tulloch, A. J., Teo, S., Carvajal, B. V., Tessier-Lavigne, M., & Jaworski, A. (2019). Diverse spinal commissural neuron populations revealed by fate mapping and molecular profiling using a novel Robo3 ^{Cre} mouse. *The Journal of Comparative Neurology*, *527*, 2948–2972. https://doi.org/10.1002/cne.24720

Yasaka, T., Tiong, S. Y. X., Hughes, D. I., Riddell, J. S., & Todd, A. J. (2010). Populations of inhibitory and excitatory interneurons in lamina II of the adult rat spinal dorsal horn revealed by a combined electrophysiological and anatomical approach. *Pain*, *151*, 475–488. https://doi.org/10.1016/j.pain.2010.08.008

Yoshida, S., Senba, E., Kubota, Y., Hagihira, S., Yoshiya, I., Emson, P. C., & Tohyama, M. (1990). Calcium-binding proteins calbindin and parvalbumin in the superficial dorsal horn of the rat spinal cord. *Neuroscience*, *37*, 839–848. https://doi.org/10.1016/0306-4522(90)90113-i

Zeilhofer, H. U., Acuna, M. A., Gingras, J., & Yévenes, G. E. (2018). Glycine receptors and glycine transporters: Targets for novel analgesics? *Cellular and Molecular Life Sciences*, *75*, 447–465. https://doi.org/10.1007/s00018-017-2622-x

Zeilhofer, H. U., Studler, B., Arabadzisz, D., Schweizer, C., Ahmadi, S., Layh, B., Bösl, M. R., & Fritschy, J. M. (2005). Glycinergic neurons expressing enhanced green fluorescent protein in bacterial artificial chromosome transgenic mice. *The Journal of Comparative Neurology*, *482*, 123–141. https://doi.org/10.1002/cne.20349

Zeilhofer, H. U., Werynska, K., Gingras, J., & Yévenes, G. E. (2021). Glycine receptors in spinal nociceptive control—An update. *Biomolecules*, *11*(6), 846. https://doi.org/10.3390/biom11060846

Zeisel, A., Hochgerner, H., Lönnerberg, P., Johnsson, A., Memic, F., van der Zwan, J., Häring, M., Braun, E., Borm, L. E., La Manno, G., Codeluppi, S., Furlan, A., Lee, K., Skene, N., Harris, K. D., Hjerling-Leffler, J., Arenas, E., Ernfors, P., Marklund, U., & Linnarsson, S. (2018). Molecular architecture of the mouse nervous system. *Cell*, *174*, 999–1014.e22. https://doi.org/10.1016/j.cell.2018.06.021

Zhang, X., Nicholas, A. P., & Hökfelt, T. (1995). Ultrastructural studies on peptides in the dorsal horn of the rat spinal cord – II. Co-existence of galanin with other peptides in local neurons. *Neuroscience*, *64*, 875–891. https://doi.org/10.1016/0306-4522(94)00451-a

Zheng, J., Lu, Y., & Perl, E. R. (2010). Inhibitory neurones of the spinal substantia gelatinosa mediate interaction of signals from primary afferents. *The Journal of Physiology*, *588*, 2065–2075. https://doi.org/10.1113/jphysiol.2010.188052

Zheng, Y., Liu, P., Bai, L., Trimmer, J. S., Bean, B. P., & Ginty, D. D. (2019). Deep sequencing of somatosensory neurons reveals molecular determinants of intrinsic physiological properties. *Neuron*, *103*, 598–616. https://doi.org/10.1016/j.neuron.2019.05.039

How to cite this article: Miranda, C. O., Hegedüs, K., Wildner, H., Zeilhofer, H. U., & Antal, M. (2021). Morphological and neurochemical characterization of glycinergic neurons in laminae I–IV of the mouse spinal dorsal horn. *Journal of Comparative Neurology*, 1–20. https://doi.org/10.1002/cne.25232